












## Article

# Fiducial Reference Measurements for Air Quality Monitoring Using Ground-Based MAX-DOAS Instruments (FRM4DOAS)

Michel Van Roozendael <sup>1,\*</sup>, Francois Hendrick <sup>1</sup>, Martina M. Friedrich <sup>1</sup>, Caroline Fayt <sup>1</sup>, Alkis Bais <sup>2</sup>, Steffen Beirle <sup>3</sup>, Tim Bösch <sup>4</sup>, Monica Navarro Comas <sup>5</sup>, Udo Friess <sup>6</sup>, Dimitris Karagkiozidis <sup>2</sup>, Karin Kreher <sup>7</sup>, Alexis Merlaud <sup>1</sup>, Gaia Pinardi <sup>1</sup>, Ankie Piters <sup>8</sup>, Cristina Prados-Roman <sup>5</sup>, Olga Puentedura <sup>5</sup>, Lucas Reischmann <sup>3</sup>, Andreas Richter <sup>4</sup>, Jan-Lukas Tirpitz <sup>6,†</sup>, Thomas Wagner <sup>3</sup>, Margarita Yela <sup>5</sup> and Steffen Ziegler <sup>3</sup>

- <sup>1</sup> Royal Belgian Institute for Space Aeronomy, Ringlaan-3, 1180 Brussels, Belgium; francois.hendrick@aeronomie.be (F.H.); martina.m.friedrich@aeronomie.be (M.M.F.); caroline.fayt@aeronomie.be (C.F.); alexis.merlaud@aeronomie.be (A.M.); gaia.pinardi@aeronomie.be (G.P.)
- <sup>2</sup> Laboratory of Atmospheric Physics, Aristotle University of Thessaloniki, 54124 Thessaloniki, Greece; abais@auth.gr (A.B.); dkaragki@auth.gr (D.K.)
- <sup>3</sup> Max Planck Institute for Chemistry, Hahn-Meitner-Weg 1, 55128 Mainz, Germany; steffen.beirle@mpic.de (S.B.); l.reischmann@mpic.de (L.R.); thomas.wagner@mpic.de (T.W.); steffen.ziegler@mpic.de (S.Z.)
- <sup>4</sup> Institute for Environmental Physics, University of Bremen, Otto-Hahn-Allee 1, 28359 Bremen, Germany; timb@iup.physik.uni-bremen.de (T.B.); andreas.richter@iup.physik.uni-bremen.de (A.R.)
- <sup>5</sup> National Institute for Aerospace Technology, Ctra. de Ajalvir, km 4, 28850 Torrejón de Ardoz, Spain; navarrocm@inta.es (M.N.C.); pradosrc@inta.es (C.P.-R.); puentero@inta.es (O.P.); yelam@inta.es (M.Y.)
- <sup>6</sup> Institute of Environmental Physics, University of Heidelberg, Grabengasse 1, 69117 Heidelberg, Germany; udo.friess@iup.uni-heidelberg.de (U.F.); jltirpitz@atmos.ucla.edu (J.-L.T.)
- <sup>7</sup> BK Scientific, 42 Astheimerweg, 55130 Mainz, Germany; karin.kreher@bkscientific.eu
- <sup>8</sup> Royal Netherlands Meteorological Institute, Utrechtseweg 297, 3731 GA De Bilt, The Netherlands; piters@knmi.nl
- \* Correspondence: michel.vanroozendael@aeronomie.be
- † Current address: Department of Atmospheric and Oceanic Sciences, Maths Science Building, University of California, Los Angeles, 520 Portola Plaza, Los Angeles, CA 90095, USA.



**Citation:** Van Roozendael, M.; Hendrick, F.; Friedrich, M.M.; Fayt, C.; Bais, A.; Beirle, S.; Bösch, T.; Navarro Comas, M.; Friess, U.; Karagkiozidis, D.; et al. Fiducial Reference Measurements for Air Quality Monitoring Using Ground-Based MAX-DOAS Instruments (FRM4DOAS). *Remote Sens.* **2024**, *16*, 4523. <https://doi.org/10.3390/rs16234523>

Academic Editor: Carmine Serio

Received: 27 September 2024

Revised: 11 November 2024

Accepted: 12 November 2024

Published: 2 December 2024



**Copyright:** © 2024 by the authors. Licensee MDPI, Basel, Switzerland. This article is an open access article distributed under the terms and conditions of the Creative Commons Attribution (CC BY) license (<https://creativecommons.org/licenses/by/4.0/>).

**Abstract:** The UV–Visible Working Group of the Network for the Detection of Atmospheric Composition Changes (NDACC) focuses on the monitoring of air-quality-related stratospheric and tropospheric trace gases in support of trend analysis, satellite validation and model studies. Tropospheric measurements are based on MAX-DOAS-type instruments that progressively emerged in the years 2010 onward. In the interest of improving the overall consistency of the NDACC MAX-DOAS network and facilitating its further extension to the benefit of satellite validation, the ESA initiated, in late 2016, the FRM4DOAS project, which aimed to set up the first centralised data processing system for MAX-DOAS-type instruments. Developed by a consortium of European scientists with proven expertise in measurements, data extraction algorithms and software design specialities, the system has now reached pre-operational status and has demonstrated its ability to deliver a set of quality-controlled atmospheric composition data products with a latency of one day. The processing system has been designed using a highly modular approach, making it easy to integrate new tools or processing updates. It incorporates advanced algorithms selected by community consensus for the retrieval of total ozone, lower tropospheric and stratospheric NO<sub>2</sub> vertical profiles and formaldehyde profiles. The ozone and NO<sub>2</sub> products are currently generated from a total of 22 stations and delivered daily to the NDACC rapid delivery (RD) repository, with an additional mirroring to the ESA Validation Data Centre (EVDC). Although it is still operated in a pre-operational/demonstrational mode, FRM4DOAS was already used for several validation and science studies, and it was also deployed in support of field campaigns for the validation of the TROPOMI and GEMS satellite missions. It recently went through a CEOS-FRM self-assessment process aiming at assessing the level of maturity of the service in terms of instrumentation, operations, data sampling, metrology and verification. Based on this evaluation, it falls under class C, which is a good rating but also implies that further improvements are needed to reach full compliance with FRM standards, i.e., class A.

**Keywords:** fiducial reference measurements; remote sensing; UV–visible; DOAS; NDACC; reactive gases

## 1. Introduction

Satellite remote sensing of the atmospheric composition has developed over the last decades with a number of missions such as GOME on ERS-2 [1], SCIAMACHY on ENVISAT [2], the Ozone Monitoring Instrument (OMI) on EOS-Aura [3], the Global Ozone Monitoring Experiment-2 (GOME-2) onboard MetOp A, B and C [4] and the TROPospheric Monitoring Instrument (TROPOMI) onboard Sentinel-5 Precursor (S5p) [5], the latter to be followed in 2025 by Sentinel-4 and Sentinel-5, respectively, onboard the EUMETSAT platforms MTG-S and METOP-SG. Sentinel 4, 5 and S5p missions are an essential component of the Copernicus Atmosphere Monitoring Service (CAMS, <https://atmosphere.copernicus.eu/>, accessed on 27 November 2024), one of the six operational services of the EU's Copernicus Programme (<https://www.copernicus.eu/en>, accessed on 27 November 2024). The CAMS relies on the Integrated Forecast System (IFS), a complex suite of atmospheric models that assimilate satellite data to produce forecasts and analyses of various reactive gases as well as aerosols and greenhouse gases.

The calibration and validation (Cal/Val) of satellite data depends largely on the availability of high-quality independent ground-based reference datasets representative of the various measurement conditions sampled by satellite sensors. With time, Cal/Val has progressively evolved from a purely research-driven activity to a more coordinated and comprehensive assessment and reporting of the quality, biases and residual uncertainty in the satellite observations, being performed in operational environments such as, e.g., the ESA S5P Mission Performance Centre (MPC) Validation Data Analysis Facility (VDAF) (<https://mpc-vdaf.tropomi.eu/>, accessed on 27 November 2024). A key requirement, formulated within the Quality Assurance Framework for Earth Observation (QA4EO), is that the independent dataset itself must be fully characterised in a manner consistent with the QA4EO process, i.e., that it has documented evidence of its level of internal consistency. This led the ESA to develop the concept of Fiducial Reference Measurements (or FRM), a label aiming to create a class of observations optimised to meet the needs of the satellite community.

The Pandonia global network (PGN, <https://www.pandonia-global-network.org/>, accessed on 27 November 2024) is an example of a recently developed atmospheric composition monitoring network based on the FRM concept. The PGN was built around the Pandora instrument [6] that was designed in the late 2000 to operationally monitor ozone and other trace gases using direct sun UV–Visible spectroscopy. Next to Pandora systems, many alternative instruments exploiting the UV–Visible Differential Optical Absorption Spectroscopy (DOAS) technique have also been developed by various research institutes and deployed worldwide for the monitoring of atmospheric trace gases such as nitrogen dioxide (NO<sub>2</sub>), ozone (O<sub>3</sub>), the collisional complex of oxygen (O<sub>4</sub>), formaldehyde (HCHO), bromine oxide (BrO) and several other species. A number of these instruments are operated within the Network for the Detection of Atmospheric Composition Change (NDACC, <https://www.ndacc.org/>, accessed on 27 November 2024). Initially constituted in the 1990s to observe and understand the physical and chemical state of the stratosphere, the NDACC (formerly the NDSC, Network for the Detection of Stratospheric Changes) has gradually expanded its focus to the study of the tropospheric composition. In the UV–Visible spectral range, tropospheric trace gases are routinely monitored using the Multi-AXis DOAS (MAX-DOAS) technique [7,8]. The quality of the retrieved products of NDACC-affiliated instruments is assessed through participation in regular intercomparison exercises, e.g., the CINDI [9] and CINDI-2 [10] campaigns. Protocols and calibration procedures have also been established to ensure network consistency and long-term stability of the generated data records. However, the UV–Vis NDACC MAX-DOAS network has been lacking

harmonisation in data retrieval approaches, and the traceability of its procedures could be improved.

Therefore, to further enhance NDACC UV–Vis capabilities towards meeting FRM requirements, the ESA initiated the FRM4DOAS project, which aims at (1) specifying calibration procedures and best practices for instrument operation and characterisation, (2) improving and harmonising retrieval algorithms applied to UV–Vis ground-based DOAS spectrometers and (3) operationally delivering consistent data products as needed for the validation of current and future atmospheric composition satellite missions. This paper describes the concept of the FRM4DOAS system and its main realisations. This includes a round-robin selection of retrieval algorithms and their integration in a centralised data processing system developed in support of the NDACC and operationally reporting NO<sub>2</sub>, ozone and HCHO data products with a typical latency of 1 day. Section 2 describes the status of the measurement network and the associated requirements. It also briefly documents the retrieval algorithms used in the system and provides a detailed description of the processing system. Section 3 addresses validation activities as well as the first results from the system operated in a demonstrational mode. Finally, Section 4 concludes with a discussion of the main outcome of the project and future challenges.

## 2. Materials and Methods

### 2.1. Instruments and Network Requirements

Although the overall measurement principle is the same for all UV–Vis DOAS systems operated worldwide, there is a wide diversity of such instruments, both in design and operation, since they are usually developed by individual research groups and institutes. Differences among instruments are primarily driven by the scientific applications for which they are developed (e.g., stratospheric research, air pollution monitoring, monitoring of volcanic emissions, power plant emission monitoring, etc.), as well as by the cost of development and ease of deployment. Such different approaches to the design and operation can become limiting factors for the establishment of a network, and this needs to be addressed when integrating instruments into a centralised processing system. Hence, FRM4DOAS provides recommendations and guidelines (best practices) for instrument operation and characterisation. In addition, as further described later, it focuses on the development of a near-real-time centralised data processing system for all participating instruments using homogenous retrieval settings. Currently, more than 20 ground-based DOAS instruments are centrally processed by FRM4DOAS. Their locations and responsible institutes are listed in Table 1.

**Table 1.** Geographical location of ground-based UV–Visible stations that operationally submit data to the FRM4DOAS processing system.

Station Name	Country	Institute Acronym	Latitude (°N)	Longitude (°E)	Altitude (m a.s.l.)
Ny-Alesund	Norway	IUP Bremen <sup>1</sup>	78.919	11.930	20
Harestua	Norway	BIRA-IASB <sup>2</sup>	60.216	10.753	600
Bremen	Germany	IUP Bremen <sup>1</sup>	53.103	8.849	46
De Bilt	Netherlands	KNMI <sup>3</sup>	52.101	5.177	22
Cabauw	Netherlands	KNMI <sup>3</sup>	51.967	4.927	3
Uccle	Belgium	BIRA-IASB <sup>2</sup>	50.799	4.360	125
Vielsalm	Belgium	BIRA-IASB <sup>2</sup>	50.305	5.998	445
Mainz	Germany	MPIC <sup>4</sup>	49.990	8.229	160
Heidelberg	Germany	IUP Heidelberg <sup>5</sup>	49.417	8.674	145
Jungfraujoch	Switzerland	BIRA-IASB <sup>2</sup>	46.547	7.985	3580
San Pietro Capofiume	Italy	CNR-ISAC <sup>6</sup>	44.650	11.619	12
Toronto Downsview	Canada	ECCC <sup>7</sup>	43.780	−79.468	221
Thessaloniki	Greece	AUTH-LAP <sup>8</sup>	40.633	22.955	80
Xianghe	China	BIRA-IASB <sup>2</sup>	39.750	116.959	95

Table 1. Cont.

Station Name	Country	Institute Acronym	Latitude (°N)	Longitude (°E)	Altitude (m a.s.l.)
Athens	Greece	IUP Bremen <sup>1</sup>	38.049	23.860	532
Izana	Spain	INTA <sup>9</sup>	28.309	−16.499	2393
Kinshasa	RD Congo	BIRA-IASB <sup>2</sup>	−4.420	15.310	450
La Reunion Maito	France	BIRA-IASB <sup>2</sup>	−21.059	55.380	2158
Lauder	New Zealand	NIWA <sup>10</sup>	−45.037	169.684	374
Neumayer	Antarctica	IUP Heidelberg <sup>5</sup>	−70.690	−8.270	48
Arrival Heights	Antarctica	IUP Heidelberg <sup>5</sup>	−77.830	166.649	192

<sup>1</sup> Institute for Environmental Physics, University of Bremen, Bremen, Germany; <sup>2</sup> Royal Belgian Institute for Space Aeronomy, Brussels, Belgium; <sup>3</sup> Royal Netherlands Meteorological Institute, Utrecht, Netherlands; <sup>4</sup> Max Planck Institute for Chemistry, Mainz, Germany; <sup>5</sup> Institute of Environmental Physics, University of Heidelberg, Heidelberg, Germany; <sup>6</sup> Institute of Atmospheric Sciences and Climate, Bologna, Italy; <sup>7</sup> Environment and Climate Change Canada, Air Quality Research Division, Toronto, Canada; <sup>8</sup> Laboratory of Atmospheric Physics, Aristotle University of Thessaloniki, Thessaloniki, Greece; <sup>9</sup> Instituto Nacional de Técnica Aeroespacial, Torrejón de Ardoz, Spain; <sup>10</sup> National Institute of Water and Atmosphere Research Centre, Lauder, New Zealand.

The requirements for MAX-DOAS systems to be used for satellite Cal/Val are primarily driven by the needs of the satellite products, both in terms of relevance and the necessary accuracy and precision of the measured quantities. The wavelength coverage of the instruments' spectrographs as well as their spectral resolution are major factors in all DOAS applications since they impact the sensitivity of the measurements and the number of species that can be retrieved.

Within FRM4DOAS, both the UV and visible ranges of the spectrum need to be covered, typically from 300 to 550 nm, so that multiple absorbers can be measured. Furthermore, high signal-to-noise ratio (SNR) measurements are required (3000–4000 depending on the target species) to provide high-quality reference ground-based datasets for the validation of satellite observations. While twilight observations at a single viewing direction (zenith) are adequate for the retrieval of stratospheric trace gas concentrations [11–13], monitoring of tropospheric trace gases requires scanning across elevation angles [7,8]. Hence, most instruments contributing to FRM4DOAS are equipped with motorised systems, characterised by a pointing accuracy better than 0.2° [14] and allowing scanning from near the horizon up to the zenith. The field of view (FOV) of the instruments should also be restricted, usually by a telescope, to typically less than 1.5°, ensuring that spectral radiances at different elevation angles do not overlap.

MAX-DOAS systems that perform elevation scans at multiple azimuthal viewing directions (2D instruments) provide an improved spatial coverage compared to one-dimensional (1D) instruments that work at a single fixed azimuth. This allows for the investigation of possible horizontal inhomogeneities and for a better characterisation of the field around the measurement site [15,16]. It should be noted that the requirements mentioned above are indicative and should not be treated as strict thresholds.

The geographical layout of an optimal MAX-DOAS validation network is determined by the spatial variability and distribution of the parameters of interest. Species with long atmospheric lifetimes, such as carbon dioxide (CO<sub>2</sub>), need fewer stations than reactive gases, such as NO<sub>2</sub>, which are characterised by high spatio-temporal variability. Thorough validation requires a spatial distribution of the ground-based measurements covering both hemispheres, all relevant latitudes from the tropics to polar regions, background regions and measurement sites where high concentrations are expected, as well as regions that are characterised by different conditions with respect to parameters that can potentially affect the quality of the measurements, such as surface albedo, topography, cloud coverage and aerosol loading. Figure 1 visualises the current geographical distribution of MAX-DOAS systems that are centrally processed by FRM4DOAS. We anticipate that this network of instruments will grow with time when the FRM4DOAS system moves into an operational phase.

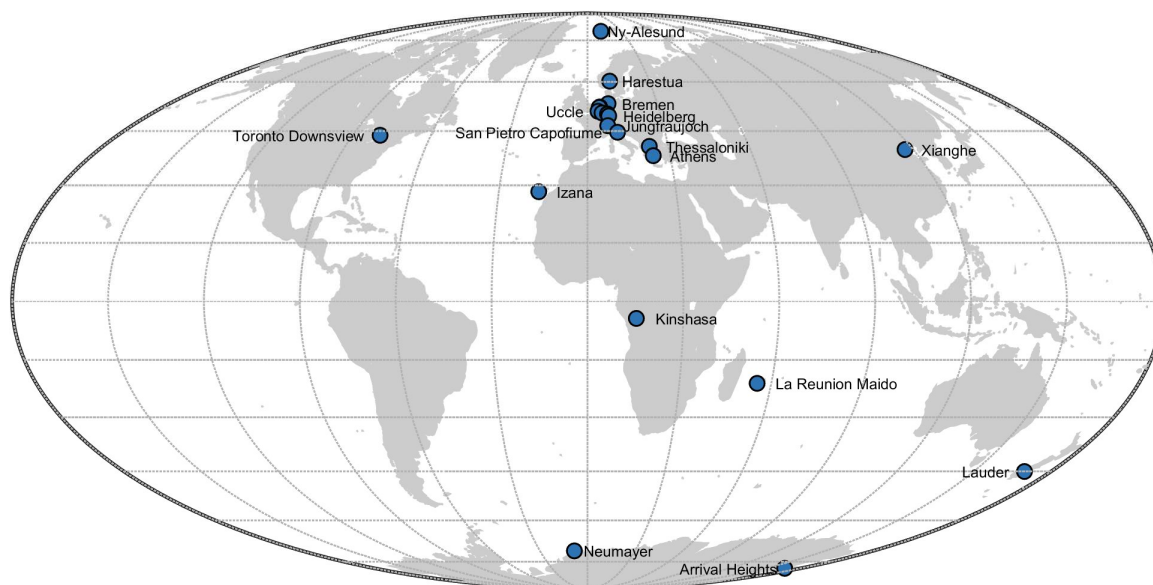


**Figure 1.** Current geographical distribution of the UV-Visible instruments that are centrally processed by the FRM4DOAS system (for more details, see Table 1).

## 2.2. Retrieval Algorithms

### 2.2.1. Round-Robin of MAX-DOAS Retrievals of NO<sub>2</sub>, HCHO and Aerosols

As part of the system design phase, an extensive assessment of the performance of retrieval algorithms for tropospheric trace gases and aerosols from MAX-DOAS measurements was performed to identify suitable retrieval algorithms for the FRM4DOAS operational processor. This retrieval round-robin included the eight different algorithms listed in Table 2, of which five were based on optimal estimation methods (OEM [17]), two parameterised approaches using lookup tables and one algorithm was based on an analytical approach. Retrievals were performed for a variety of different synthetic profiles of NO<sub>2</sub>, HCHO and aerosol profiles, allowing for a quantitative comparison of true and retrieved profiles. These scenarios included exponential profiles and box profiles of different heights, as well as uplifted layers and two cloud cases, yielding in total of 110 different combinations of trace gases and aerosol scenarios. For each scenario, a set of differential slant column densities (dSCDs) was simulated by each of the forward models of the participating retrieval algorithms for a viewing angle sequence consisting of ten elevation angles from 1° to 90°. The median from all forward models then served as the reference dSCD dataset that represented the input for the retrieval algorithms. In addition to retrievals without any noise (dataset v1), retrievals with typical levels of artificial noise (dataset v1n) were also performed. Retrieval settings, including aerosol optical properties and the specifications of the layer grid, were prescribed.

**Table 2.** MAX-DOAS retrieval algorithms participating in the retrieval round-robin. OEM: optimal estimation; PAR: parameterised retrieval based on lookup tables; ANA: analytical approach.

Algorithm	Institute	Method	Reference
bePRO	BIRA-IASB	OEM	[18]
BOREAS	IUP Bremen	OEM	[19]
HEIPRO	IUP Heidelberg	OEM	[20]
MMF	BIRA-IASB	OEM	[21]
PRIAM	MPIC	OEM	[22]
MAPA	MPIC	PAR	[23]
MARK	KNMI	PAR	[24]
NASA	NASA <sup>1</sup>	ANA	Blick Software Suite Manual, version 1.8 <sup>2</sup>

<sup>1</sup> NASA-Goddard, Greenbelt, United States; <sup>2</sup> <https://www.pandonia-global-network.org/home/documents/manuals/>, accessed on 27 November 2024.

Since the results of this retrieval round-robin were already published [25], we present only a summary here. Results of the comparison of AODs and trace gas vertical column densities (VCDs) are shown in Figure 2. Generally, good agreement between true and retrieved aerosol and trace gas profiles was found for most of the models. Retrieved surface values of aerosol extinction and trace gas concentrations deviated from the truth by  $(0.08\text{--}0.25) \text{ km}^{-1}$  and  $(5.9\text{--}15.0) \times 10^{10} \text{ molec cm}^{-3}$  (or about 2.4–6 ppb), respectively.

The most suitable retrieval algorithms both in terms of computational performance and accuracy turned out to be the MMF algorithm based on optimal estimation as well as the MAPA algorithms based on a fast parameterised approach using lookup tables. It was therefore decided to implement these two algorithms into the FRM4DOAS operational processor. This allows for a cross-validation of both algorithms on an operational basis. Furthermore, the validity of the retrieval products can be assessed based on the level of agreement of both algorithms. See [25] for a comprehensive description of the results of this retrieval round-robin, which also includes a discussion of uncertainties. We estimate the uncertainty on the tropospheric  $\text{NO}_2$  column to be of the order of 15%; however, this number can be strongly modulated depending on the aerosol content, its vertical distribution and the geometry of the observations.

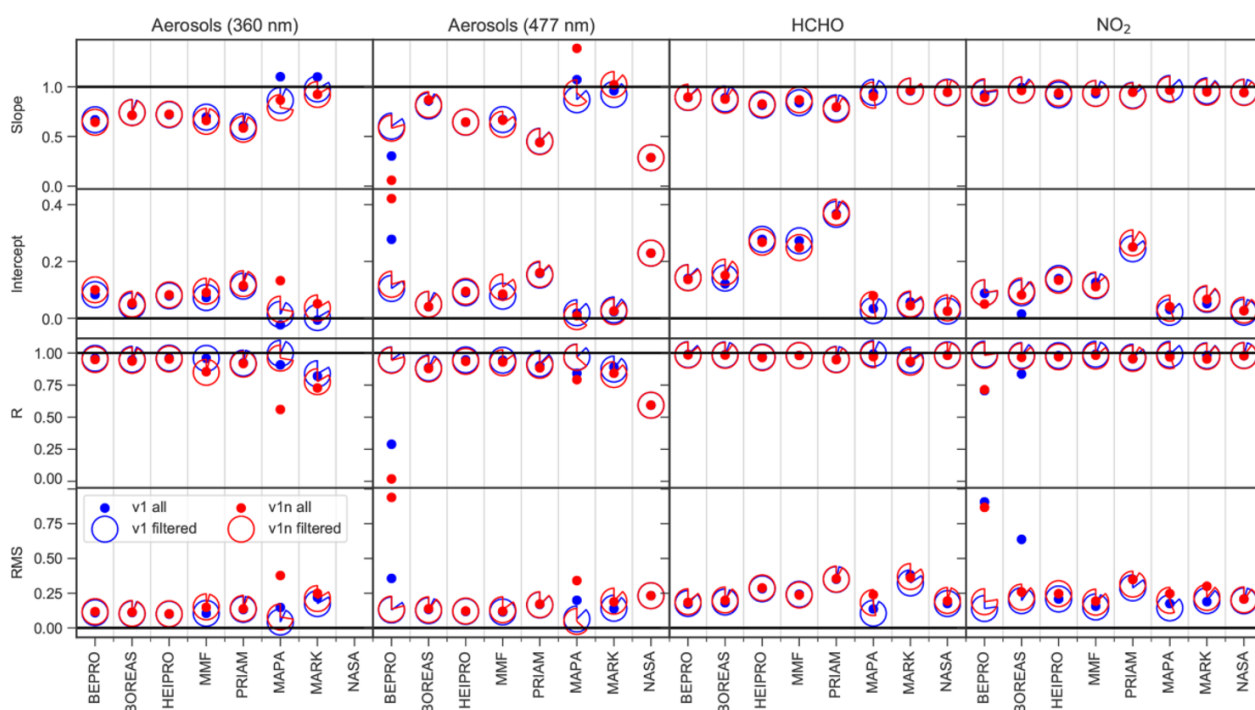


**Figure 2.** From top to bottom: slope, intercept, regression coefficient and root mean squares (RMSs) of a linear regression between true and retrieved total aerosol optical thickness derived from  $\text{O}_4$  dSCDs at 360 nm and 477 nm and HCHO and  $\text{NO}_2$  tropospheric total columns for each of the algorithms. Dots show all data; circular symbols represent pie charts that quantify the fraction of data flagged as valid. Intercept and RMS values are in dimensionless units for aerosols and  $10^{16} \text{ molec cm}^{-2}$  for HCHO and  $\text{NO}_2$ . This figure is adapted from (Figure 18 in [25]).

### 2.2.2. Total Ozone Retrieval

Total ozone column is retrieved from zenith-sky twilight observations using the NDACC standard approach described in [13]. The procedure involves two steps. The first one consists of obtaining the gas density along the optical path or differential slant column density (dSCD) by means of a DOAS spectral fitting. In FRM4DOAS, this spectral fit is based on the QDOAS software, version 3.4.7, 3 February 2021 [26]. The DOAS parameters for  $\text{O}_3$  dSCD retrieval are defined according to [13] with some adaptations reflecting recent updates in spectroscopy and new practices to account for temperature dependence effects.

The settings currently adopted for FRM4DOAS are given in Table 3. They include specifications for the spectral fitting range, the absorption cross sections of the active gases in the chosen spectral range and some operational parameters for the DOAS fitting.

**Table 3.** Spectral retrieval settings for ozone in the Chappuis band.

Wavelength range	450–540 nm
Wavelength calibration method	Based on the reference solar atlas of Chance and Kurucz [27]
Absorption cross-sections:	
O <sub>3</sub> (223 K and 243 K)	[28]; 243 K orthogonalised to 223 K
NO <sub>2</sub> (220 K and 298 K)	[29]; 298 K orthogonalised to 220 K; I <sub>0</sub> effect-corrected
O <sub>4</sub> (293 K and 203 K)	[30]; 203 K orthogonalised to 293 K
H <sub>2</sub> O	[31]
Ring effect	Pseudo-absorber [32,33]
Polynomial	Order 5 (6 coefficients)
Intensity offset correction	Order 1

The second step is the conversion of the dSCD into a vertical column density (VCD), which directly follows [13]. For the selection of the solar zenith angle (SZA) range representative of twilight conditions, the best compromise between accuracy and precision is achieved in the 86–91° SZA range. The retrieved VCD is obtained at an effective SZA, which is usually fixed at 90°.

For zenith-sky twilight observations, the observed air mass is not exactly located over the observation site, but it is horizontally shifted towards east in the morning and towards west in the evening. The average horizontal displacement can reach up to 500 km from the station in the stratosphere during twilight. This horizontal displacement must be considered to make a correct comparison with satellite measurements. In the FRM4DOAS processing system, lookup tables (LUTs) of the horizontal displacement depending on SZA angle and altitude are used in combination with the solar azimuth angle to report the mean location of the effective air mass corresponding to the total O<sub>3</sub> columns and stratospheric NO<sub>2</sub> profile.

Sources of uncertainties in zenith-sky twilight total ozone retrievals are documented in [13]. They mainly originate from random errors associated with the fitting procedure, systematic uncertainties related to the ozone absorption cross-sections and pseudo-random errors related to the calculation of the air mass factor that is used to convert dSCDs into VCDs. The overall uncertainty on the vertical column derivation is estimated to be 5.9% at 90° SZA. Note that clouds have a small impact on zenith-sky ozone measurements at twilight, which is an advantage of the technique. Another advantage is the possibility of measuring under most weather conditions (excluding fog and heavy rain) and at all latitudes even in polar regions.

### 2.2.3. Stratospheric NO<sub>2</sub> Vertical Profiling

The vertical distribution of stratospheric NO<sub>2</sub> can be retrieved from ground-based measurements of the zenith-scattered sunlight. Basically, at visible wavelengths where NO<sub>2</sub> absorption is measured, the mean altitude at which Rayleigh scattering occurs increases with increasing SZA. During twilight, the mean scattering altitude scans the stratosphere rapidly, yielding height-resolved information on the absorption by stratospheric NO<sub>2</sub> (see Figure 3). Through linear optimal estimation (OEM), vertical profiles of stratospheric compounds can be derived from zenith-sky DOAS observations at twilight [12,34].

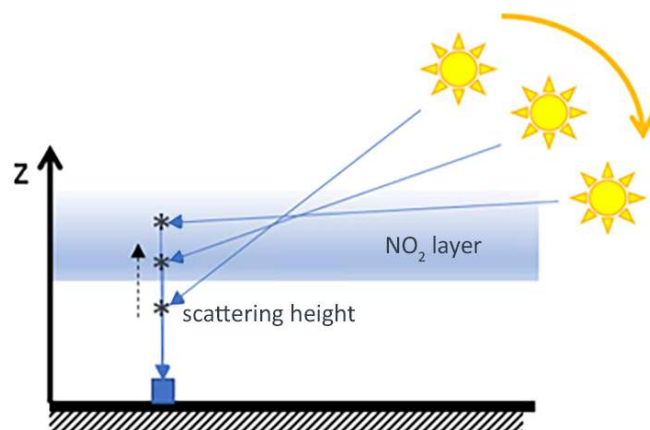


**Figure 3.** Twilight zenith-sky geometry used for stratospheric trace gas vertical profile retrievals. As indicated, the mean scattering altitude depends on the solar elevation.

The algorithm implemented in the FRM4DOAS system is based on the work by [12]. It allows for retrieving sunrise and sunset  $\text{NO}_2$  stratospheric profiles in the altitude range of 20–40 km, representative of conditions at  $90^\circ$  SZA. The details of the OEM algorithm are described in [12], and therefore, only a summary of its main features is presented here, with a focus on deviations resulting from the FRM4DOAS implementation.

As for ozone retrievals, the first step of the evaluation consists of a spectral fitting using the QDOAS algorithm to produce dSCDs. Settings currently adopted for FRM4DOAS are given in Table 4.

**Table 4.** Spectral settings used for stratospheric  $\text{NO}_2$  retrieval in the visible range.

Wavelength range	425–490 nm (alternative ranges: 411–445 nm or 445–490 nm)
Wavelength calibration method	Based on reference solar atlas of Chance and Kurucz [27]
Absorption cross-sections:	
$\text{O}_3$ (223 K)	[28]
$\text{NO}_2$ (220 K and 298 K)	[29]; 298 K orthogonalised to 220 K; $I_0$ effect-corrected
$\text{O}_4$ (293 K)	[30]
$\text{H}_2\text{O}$	[31]
Ring effect	Pseudo-absorber [32,33]
Polynomial	Order 3 (4 coefficients)
Intensity offset correction	Order 1

The second step consists of retrieving stratospheric  $\text{NO}_2$  profiles from the measured dSCDs. The profiling algorithm applied in FRM4DOAS is based on the OEM and is fully described in [12]. To reproduce the rapid variation of  $\text{NO}_2$  at twilight, the forward model includes a stacked box photochemical model (PSC-Box [35]) initialised with meteorological and chemical fields at the location of the station obtained with the 3D-CTM SLIMCAT [36]. Based on these simulations,  $\text{NO}_2$  slant columns (and corresponding weighting functions) are calculated using the pseudo-spherical radiative transfer model UVSPEC/DISORT [37], which has been validated in several past studies [38,39]. To provide the FRM4DOAS processing system with the capability to retrieve  $\text{NO}_2$  stratospheric vertical profiles at globally distributed stations, a set of LUTs of weighting functions (WFs) were calculated for  $10^\circ$  latitude bands between  $90^\circ\text{S}$  and  $90^\circ\text{N}$ .

Although the core of the algorithm remains identical to the one described in [12], recent developments described in the FRM4DOAS technical documentation (<https://frm4doas.aeronomie.be/index.php/documents/deliverables>, accessed on 27 November 2024) but not yet implemented in the current version of the processor have led to major improvements in the stability of the retrievals. In particular, it was shown that improved retrievals can



be obtained when reducing the NO<sub>2</sub> photolysis rate by 10% (which is within the known uncertainty range of this parameter) in the PSCBOX/SLIMCAT chemical model runs.

Uncertainties on NO<sub>2</sub> are both systematic and random in nature. While systematic errors are mostly driven by uncertainties in the NO<sub>2</sub> absorption cross-sections and their temperature dependence (2–4%), main error sources come from uncertainties in the forward model parameters. More details on the estimation of these uncertainties are given in [12].

#### 2.2.4. Cloud Detection and Flagging

As clouds massively affect the atmospheric light paths, MAX-DOAS measurements under cloudy conditions can generally not be used for profile retrievals (see Table 5). Thus, reliable cloud information is required to flag cloudy MAX-DOAS measurements as dubious or invalid. Beyond simple flagging, a cloud classification algorithm allows for investigation of the effects of different cloud conditions for MAX-DOAS profile measurements separately. The determination of cloud properties from MAX-DOAS measurements themselves (instead of using independent cloud information) has several advantages. First, the cloud information can directly be assigned to the MAX-DOAS trace gas measurements without spatio-temporal interpolation. Second, the cloud algorithm can be used for MAX-DOAS measurements at different locations and with different availability of independent cloud information in a consistent way. Third, for situations with broken clouds, it might be possible to identify cloud contamination at individual elevation angles. Such cloud-contaminated measurements might then be excluded from the profile inversion.

**Table 5.** Impact of various cloud conditions on the quality of aerosol and trace gas results derived from MAX-DOAS observations. Filled circles: use of measurement is recommended. Open circles: use of measurement is not recommended. Table taken from [40].

	AOD	Aerosol Extinction near Surface	Profile of Aerosol Extinction	VCD	VMR near Surface	Profile of VMRs
Low aerosol	●	●	●	●	●	●
High aerosol	●	●	●	●	●	●
Cloud holes	○	●	○	●	●	●
Broken clouds	○	●	○	●	●	●
Continuous clouds	○	●	○	●	●	●
Fog	○	○	○	○	○	○
Thick clouds	○	○	○	○	○	○

Clouds generally have a strong impact on the radiative transfer in the atmosphere. Thus, several quantities measured by the MAX-DOAS instruments that are affected by clouds can in turn be used for deriving cloud information. The main effects are the following:

**Clouds are bright:** Clouds typically increase the radiance. However, e.g., in case of thick thunderstorm clouds, they might also decrease the radiance. Thus, the radiance alone cannot be used to non-ambiguously identify clouds.

**Clouds are white:** The clear sky has a strong wavelength dependency for scattering probability (Rayleigh scattering), while scattering on cloud particles reveals almost no wavelength dependency. Thus, clouds look white. This effect on the broadband wavelength dependency of the radiance can be quantified by a colour index (CI), i.e., the ratio of radiances for two different wavelengths. It has, however, to be noted that only in zenith view, clouds lead in general to a whitening of the sky. In non-zenith viewing directions, depending on the viewing geometry, the cloudy and clear sky can in principle have the same colour.

**Clouds alter the light path:** As clouds alter atmospheric light paths, they directly affect the measured spectral signatures of “light path proxies” like the O<sub>4</sub> SCD; also, the strength of the “Ring effect” is affected by clouds. However, as for the radiance, clouds

might increase or decrease these quantities, depending on viewing geometry, sun position and cloud height.

Since cloud conditions within the field of view of a MAX-DOAS telescope usually vary on short time scales (except for stratiform cloud cover), rapid changes in any of the quantities listed above indicate the appearance or disappearance of clouds or a change in cloud properties.

Cloud classification algorithms have been presented in different studies. Takashima et al. [41] use a simple criterion to screen cloudy scenes based on a CI, using the wavelengths 500 nm and 380 nm. A simple cloud flag is defined with a CI value above 1.5, whereby the SZA dependence of the CI for cloud-free sky is ignored. In addition, Takashima et al. [41] calculate a cloud-base height based on relative humidity derived from the H<sub>2</sub>O profiles retrieved with MAX-DOAS.

Gielen et al. [42] present a “simple and versatile cloud-screening method for MAX-DOAS retrievals”. Three different flags are derived:

- a. Sky condition flag, derived from the CI, classifies a 90° measurement as either “good”, “mediocre” or “bad” (Figure 4).
- b. A broken cloud flag, derived from rapid changes in the CI.
- c. A multiple scattering flag, derived from rapid changes in the O<sub>4</sub> DSCD (30–90°), is needed to identify clouds in presence of high aerosol load.

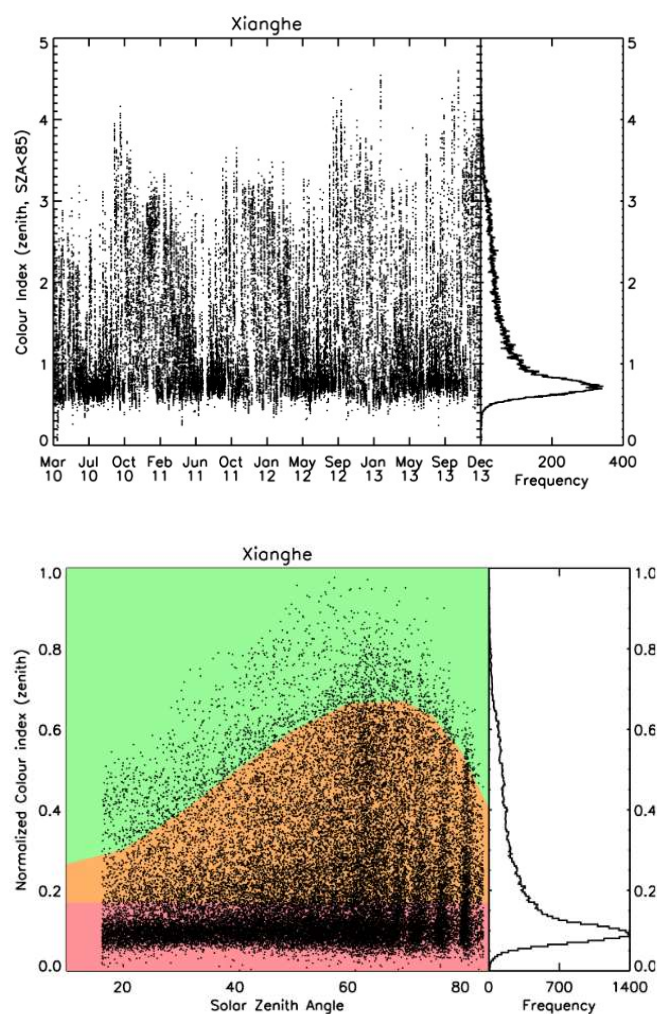


**Figure 4.** Top: Zenith CI values and frequency distribution for Xianghe. Bottom: the normalised CI values (points) versus SZA. The green, orange and red regions correspond to the “good”, “mediocre” and “bad” regions as defined by the sky flag. Figures taken from [42].

Generally, these flags can all identify clouded scenes, as demonstrated by comparisons with cloud cover determined in the thermal IR. The cloud flags were derived for three different instruments under different atmospheric conditions, and the CI was defined differently for all three instruments. The sky condition flag requires radiative transfer calculations for each CI definition to account for the SZA dependency, and the measured time series needs to be sufficiently long to be able to normalise the CI between the extremes (maximum: cloud-free; minimum: clouded).

Wagner et al. [43] presented a multi-step cloud classification scheme to categorise the cloud conditions for individual MAX-DOAS elevation sequences. The classification identifies clear sky conditions based on the absolute value of the CI at zenith and uses its temporal variability to detect rapid changes in cloudiness, corresponding to clear sky between clouds or broken clouds. The variability of the CI with elevation angles is used to detect continuous clouds (low variability) or clear sky conditions with high aerosol load (high variability, while CI at zenith varies smoothly with time). In addition, in case of a low CI, the O<sub>4</sub> SCD and its elevation angle dependency are used to detect thick clouds and fog, respectively. The full scheme is shown in Figure 5.

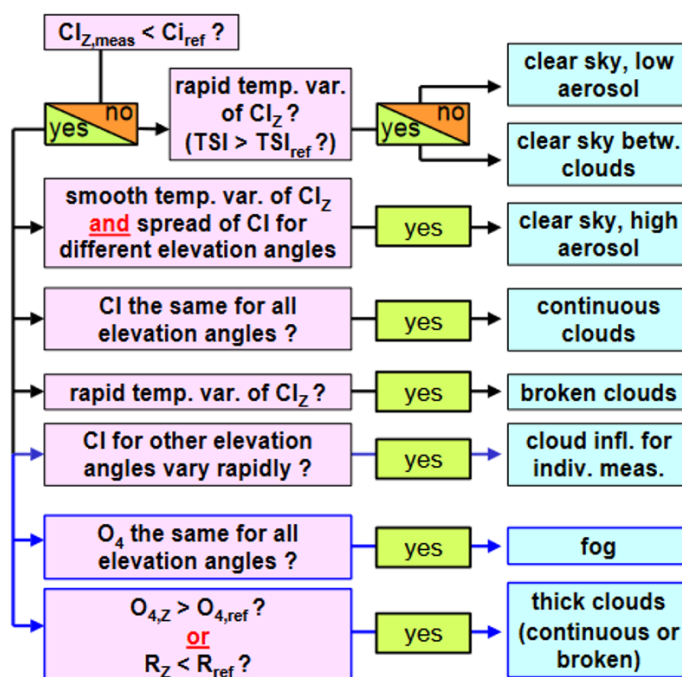


**Figure 5.** Cloud classification scheme. Paths with black arrows indicate the primary classification results: Only one primary classification result can be attributed to a given elevation sequence. Paths with blue arrows indicate secondary classification results, which complement the primary classification results. Figure taken from [43].

This algorithm has been demonstrated to successfully classify various cloud conditions from the MAX-DOAS measurements themselves. However, the given thresholds for the CI have to be derived separately for each specific instrument. An application of the cloud classification scheme to measurements from a different instrument required several modifications [44]. As for the algorithm of Gielen et al. [42], and also for the algorithm by Wagner et al. [43], the measured time series needs to be sufficiently long in order to provide good statistics for the different cloud conditions. A few years later, Wagner et al. [45] presented an updated cloud classification scheme. It is generally based on the scheme presented in [43] but now includes absolute calibration procedures for the CI and the O<sub>4</sub> SCDs based on Radiative Transport Model (RTM) calculations under well-defined atmospheric conditions and viewing geometries. With these calibrations, the cloud classification scheme is applicable to any MAX-DOAS measurement time series.

Within the FRM4DOAS project, it was therefore decided to use this cloud classification scheme. However, since this algorithm has so far only been applied to a few MAX-DOAS measurements, further tests and adjustments are still necessary and are currently ongoing. Once tested and verified, the resulting cloud classification algorithm will be implemented in the FRM4DOAS processor.

The cloud classification algorithm can in principle be applied in all climatic zones worldwide. However, there are two restrictions which are mainly important for measurements at high latitudes. First, especially in winter, the solar zenith angles at such locations will be rather high and might not cover the SZA ranges needed for the calibration procedures. Second, for measurements above high surface albedo due to snow or ice, the threshold values, especially for  $O_4$ , would have to be adapted (for more details see [45]).

### 2.3. Central Data Processing System

The FRM4DOAS project has achieved a significant milestone by developing the first central near real-time (NRT, 24 h latency) processing system for measurements from MAX-DOAS-type instruments. As indicated in previous sections, the system incorporates advanced retrieval algorithms for lower tropospheric and stratospheric  $NO_2$  vertical profiles, lower tropospheric formaldehyde vertical profiles and total ozone columns.

The system is implemented in an event-driven fashion using a succession of asynchronous modules combining bash scripts, Fortran programs and Python code. The execution of these modules is managed by independent entities. This modular design allows modules to function independently from each other and enables the seamless integration of new tools or updates. Event-driven in this context means that the arrival of a new file triggers the processing at any given stage through trigger lists (TLs). Currently, the system is designed to ingest spectra files that cover at most 1 local day of measurements. Except for the tropospheric module, all other modules need less than a minute to process a single daily file on a single processor. These modules are run on the BIRA-IASB compute servers. Due to the heavier computation for the tropospheric module, this module runs on a local super-computing facility (SPACEPOLE HPC, total available cores: 2688) and ensures that a typical daily file can be processed in a few minutes using up to 6 cores for a single file.

Below, we first describe the general workflow of the processing system (Section 2.3.1), then the general concept of a module including the log- and history file production (Section 2.3.2); a short description of each separate module follows in Sections 2.3.3–2.3.7. Finally, the description of the submission of the level-2 GEOMS HDF4 files from the FRM4DOAS database to the NDACC data handling facility and to the ESA Validation Data Centre (EVDC), as well as an overview of the current processing status, are given in Section 2.3.8.

#### 2.3.1. General Workflow of the Processing System

The processing chain is visualised by a workflow diagram in Figure 6. Circles represent files (yellow circles represent level-2 standard GEOMS format files, cyan circles represent master level-2 netCDF4 files, grey circles represent intermediate internal files and green incoming/archived level-1 files); dark blue pentagrams are processing steps (so-called modules) and (pink) parallelograms are decision stages.

The workflow can be described as follows:

- (1) A file submitter uploads a calibrated spectrum file to the FTP server. A CDL (network Common Data form Language, <http://cfconventions.org/cf-conventions/cf-conventions.html>, accessed on 27 November 2024) representation of such a file can be found at <https://frm4doas.aeronomie.be/>, accessed on 27 November 2024. During the next year, this FTP server will be replaced by a Web-based Distributed Authoring and Versioning (WebDav) server.
- (2) A process is running every 15 min on the BIRA-IASB servers to check for new files on the FTP servers. If new file(s) have arrived, they are downloaded to BIRA-IASB file

- servers, and their names are written into a trigger list (TL.Level1.check) for further processing.
- (3) A process is running every 15 min to check the trigger list TL.L1.check. If a new entry is found, information about the instrument in question is extracted from the file name and the metadata of the file. With the help of this information, corresponding configuration files are loaded. The file is checked for consistency and archived as “rejected” if the check failed or otherwise as Level1.QAQC. This checking constitutes the first module, the LEVEL1.check. It consists of checking whether all compulsory variables and attributes are present and whether the units are suitable. However, the conversion from L0 to calibrated L1 files lies in the responsibility of the data submitter. Lastly, the name of the checked file is written into a new trigger list or in two trigger lists (TL.QDOAS.S and/or TL.QDOAS.T for stratospheric and tropospheric processing, respectively), depending on the configuration file loaded. For example, the configuration file for an instrument channel operating in the UV wavelength region will indicate to only write the file name of the file in the TL.QDOAS.T trigger list because only tropospheric processing will be performed.
  - (4) (3a/b) A process is running every 15 min checking the trigger lists TL.QDOAS.S and TL.QDOAS.T. If there are new entries in either of the lists, corresponding configuration files are loaded, and the file is processed with the QDOAS software package [26], producing QDOAS.S and/or QDOAS.T output files. Details about the settings optimised for stratospheric (CONFIG.QDOAS.S) are summarised in Tables 3 and 4 (see Section 2.2.2). Directly after file production, a quality check is performed on the files and new QDOAS.S./T.QAQC files are created. Finally, the name(s) of the output file(s) are written into one or several of the following trigger lists: TL.TROPO.profiling (following the module TL.QDOAS.T.check), TL.O3total.VCD and TL.NO2strato.profiling (both following the module TL.QDOAS.S.check).
  - (5) A process is running every 15 min checking the trigger list TL.O3total.VCD. If a new entry is found, the file is analysed by the O3.total.profiling module using the appropriate configuration files for the current instrument. A QAQC check on the quality of the processing is included in this process. Directly after producing what we call the “master level-2 output file” in CF-netCDF4 format, standard GEOMS files in hdf4 format are produced (indicated as process 4.1 in Figure 6). While this is not a separate module in the sense that it is handled via trigger lists, it can be called independently without the need to perform process 4 from the start.
  - (6) A process is running every 15 min checking the trigger list TL.NO2strato.profiling. If a new entry is found, the file is analysed by the stratospheric NO<sub>2</sub> processing module using the appropriate configuration files for the current instrument. A quality check is performed at the end of the processing module. Directly after producing the corresponding master level-2 output file, standard GEOMS files in hdf4 format are produced (5.1 in Figure 6). As for the ozone module, this is not a stand-alone module but can still be processed independently if needed.
  - (7) A process is running every 5 min checking the trigger list TL.TROPO.profiling. If a new entry is found, the file is copied to an HPC (high-performance computing) cluster, and corresponding configuration files are loaded and processed by the tropospheric processing module. A CDL representation of the master level-2 file can be found at <https://frm4doas.aeronomie.be/>, accessed on 27 November 2024. A quality check is included at the end of the tropospheric processing module. As for modules (4) and (5), this is directly followed by the creation of standard GEOMS files in hdf4 format. If more than 1 trace gas were analysed, as is usually the case for channels covering the UV wavelength region, a separate GEOMS file is produced for each trace gas. Currently, NO<sub>2</sub> and HCHO are processed (6.1 and 6.2 in Figure 6), but only NO<sub>2</sub> GEOMS files are passed to the NDACC server, see Section 2.3.8.

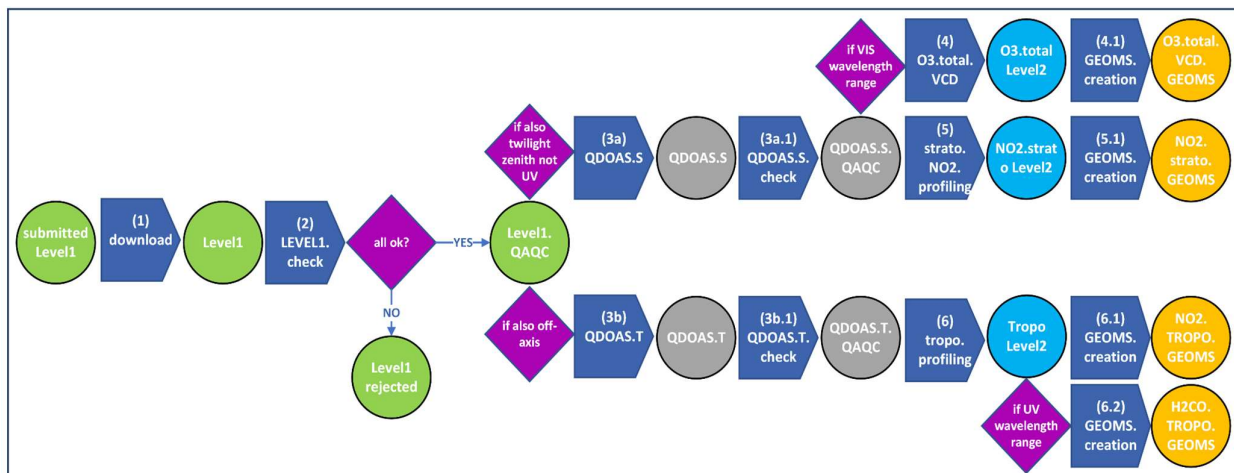


**Figure 6.** The workflow diagram of the FRM4DOAS processing system. Circles represent files (green are level-1 files, grey are internal files, cyan are master netCDF4 level-2 files, orange are level-2 files in standard GEOMS hdf4 format), dark blue pentagons represent processing steps and magenta diamond-shapes are decision steps.

While the checking intervals for Level-1.check, QDOAS, NO2.strato.profiling and O3.total.VCD are all equal to 15 min, they are slightly shifted to minimise the waiting time between processing. Each of these modules takes less than a couple of minutes to finish; hence, a shift of 2–3 min is sufficient. Likewise, the reduction in the interval for the tropo.profiling module is also motivated by optimising the total processing time.

To ensure easy back-tracing of the data throughout the processing chain, there is a specific naming convention for the files. The naming of the submitted level-1 file follows this structure:

ESA-FRM4DOAS-L1-INSTITUTE-STATIONNAME-INSTRUMENTNUMBER-CHANNELNUMBER-STARTDATE-STOPDATE-FILEVERSION.nc

The entries are defined as indicated in Table 6.

**Table 6.** Field of the file name for the level-1 files.

Institute	Name of the institute to which the instrument is affiliated.
Stationname	Name of the station, usually a city/town name.
Instrumentnumber	A specific 4-digit identifier given to each instrument submitting data to FRM4DOAS.
Channelnumber	A 1-digit number specifying the channel, usually for different spectrometers, but can also be used for different viewing directions for instruments that look in multiple viewing directions at the same time.
Startdate (stopdate)	Time of the beginning (end) of the first (last) measurement included in the file in UT. The format is YYYYMMDDTHHMMSSZ
Fileversion	Version of the file submitted, a 3-digit number preceded by “fv”.

Each following processing step adds an entry after “L1”, separated with a dot (.). Hence, the names for the quality-controlled level-1 files, QDOAS and quality-controlled QDOAS (both internal files only) are as follows:

ESA-FRM4DOAS-L1.QAQC-INSTITUTE-...-FILEVERSION.nc, ESA-FRM4DOAS-L1.QAQC.QDOAS-INSTITUTE-...-FILEVERSION.nc and ESA-FRM4DOAS-L1.QAQC.QDOAS.QAQC-INSTITUTE-...-FILEVERSION.nc, respectively.

Although the actual start and end time of measurements that are used during the total ozone processing, stratospheric NO<sub>2</sub> profiling and tropospheric trace gas profiling

might deviate (starting time of used measurements might be later and ending time of used measurements might be earlier), the original times in the file names are kept. For those three modules, the strings added after “QDOAS.QAQC” are “O3STRATO”, “NO2STRATO” and “TROPO”, respectively.

### 2.3.2. The Concept of an FRM<sub>4</sub>DOAS Module

As already indicated in Section 2.3.1, the arrival of a new file triggers the start of the process, and this is managed via trigger lists and independent entities that we call wrappers. In Figure 7, we show a conceptual diagram of a module. The module wrapper (indicated by the brown-bordered circle) runs every 15 min (every 5 min for the TROPO profiling module) and checks the module’s trigger list for new entries. If new entries are found, information about the instrument and channel number is extracted from the file name, and based on this, the correct instrument configuration file(s) are extracted from the pool of instrument-specific module configuration files. This, together with the input file in question, is passed to the module, and the module is started, loading further general module configuration files.

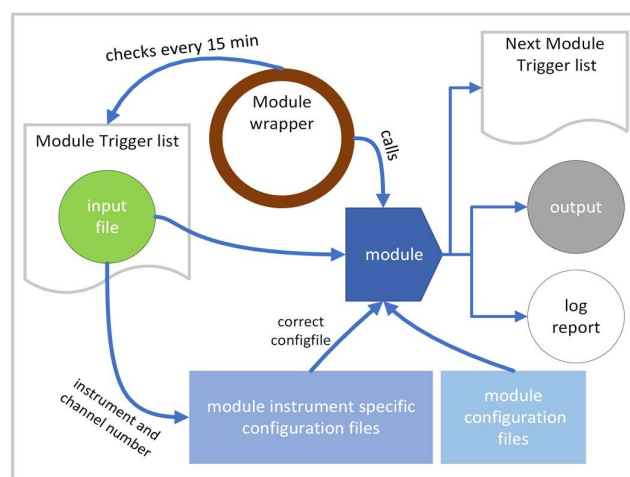


**Figure 7.** Concept diagram of an FRM<sub>4</sub>DOAS module. See main text for more details.

During the processing, warnings and errors are reported and gathered in log files that are saved and eventually archived. If no major errors occur, an output file is produced, and the name of this file is registered in the trigger list of the following module.

While most of the modules themselves are implemented in Python version 3.9 (except for the core MMF algorithm and QDOAS (version 3.4.7), which are implemented in Fortran90 and C/C++ standard, respectively), the module wrappers are implemented as bash scripts.

All log files concerning a specific level-1 file are gathered in a short report, including all warnings that occurred during any step of the processing, and sent via email to the data provider either daily, weekly or monthly, as chosen by the data provider.

### 2.3.3. The Level-1 File and the Level-1 QAQC Module

The starting point of the processing is the submission of a daily (the maximum time period that the system can ingest is currently one local day) spectra file in a specific CF-compliant netCDF4 format. These spectra (level-1) are expected to be corrected for dark current and offset. A CDL representation of the current level-1 netCDF4 file format is given at <https://frm4doas.aeronomie.be/>, accessed on 27 November 2024. The structure of this file is inspired by formats for satellite data and was designed in such a way that data providers have the possibility to deliver ancillary information that can be used in the tropospheric profiling algorithms (e.g., temperature and pressure, surface albedo or aerosol parameters such as single scattering albedo, asymmetry factor of the aerosol optical depth at a reference wavelength). This extra information will also be included in all the master level-2 netCDF4 output files. The first module consists of a file check of the level-1 files.

This check consists of the following components:

- (1) Check against an XML template whether the file structure is correct and mandatory variables and attributes are present and have expected dimensions and fill-values.
- (2) Check whether the file name is consistent with the attributes within the file
- (3) If optional variables are present, check for consistency of expected dimensions and fill-values.
- (4) If solar angles are not present, calculate solar angles from location and UTC; otherwise, check for consistency
- (5) Basic checks on measurement type (zenith, off-axis, almucantar, horizon, direct sun); details are described below
- (6) If the configuration file states that tropospheric profiling should be performed, identify elevation scans and add scan numbers and a zenith before and/or after for each scan; details are described below.

Measurement types are encoded using integers, and recognised encoded types are summarised in Table 7. As mentioned above under point 5, a basic check of these measurement types is performed. These checks are schematically illustrated in Figure 8. Such changes are never enforced, and differences between the check and the reported measurement type are only reported in the log file as a warning. Specifically, only the following changes are reported: originally classified almucantar (7) newly classified as direct sun (2) or horizon (11); originally classified as horizon (11) newly classified as almucantar (7), as well as changes that were originally classified as off-axis (1) and receive a different classification following the classification scheme outlined in Figure 8. Changes that originally have a classification different from off-axis (1) and result in a classification as possibly off-axis (1) are never reported as a warning since the classification as off-axis is never considered final. The limits in Figure 8 are specified in Table 8.

**Table 7.** Recognised measurement types and their integer value encoding.

Integer	Measurement Type
1	off-axis
2	direct sun
3	zenith
7	almucantar
11	horizon

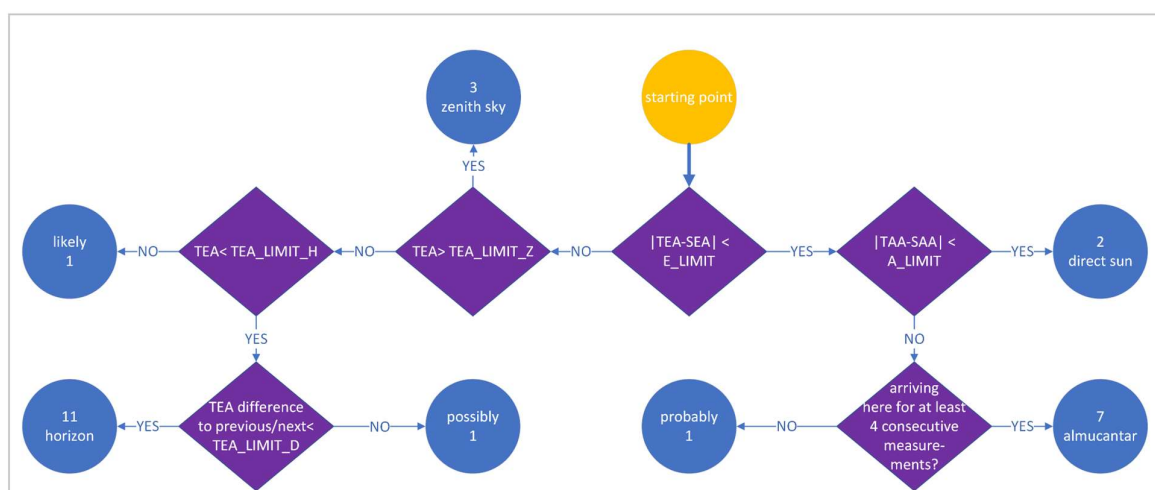


**Figure 8.** Decision tree for potential measurement type. Note that measurement type 1 (off-axis measurement) is never assigned as definite. Only certain differences between originally reported and newly classified will be flagged as a warning (7 → 2 or 11, 11 → 7); others will not be flagged. Measurement types are never changed. Current limits are given in Table 8.



**Table 8.** Limits for measurement classification.

Limit Name	Value/°
E_LIMIT	0.7
A_LIMIT	0.7
TEA_LIMIT_Z	86
TEA_LIMIT_H	2
TEA_LIMIT_D	0.25

Elevation scans and zenith reference measurements before and/or after the scan (see point 6 above) are identified following these steps:

- (1) Check if the measurements are ordered chronologically. If not, order the measurements chronologically.
- (2) Look at each set of off-axis (measurement type 1, see above) measurements between two consecutive zenith (measurement type 3) measurements.
- (3) Distribute each such set into subsets according to their telescope azimuth angle (TAA); treat azimuth angles that differ less than 1 degree as the same azimuth angle.
- (4) For each such subset, check if all measurements in the set are within a maximum time difference. Currently, this time difference is set to 40 min.
- (5) Check if each subset (after applying the maximum time difference) contains at least 2 measurements. Discard all sequences that are shorter than 2 measurements.

As is apparent from above, no check on duplicated elevation angles is performed nor is it required that the elevation angle sequence is monotonically increasing or decreasing. This choice was taken to maximise the number of scans, even in the event of motor issues or different conventions used by different groups. However, current plans to include sophisticated cloud classification schemes (see Section 2.2.4) demand a more stringent definition of an elevation scan. Hence, this assignment of scans is subject to near-future changes.

#### 2.3.4. The QDOAS Processing Module

Since the end of 2019, QDOAS [26] is part of the Atmospheric Toolbox (<https://atmospherictoolbox.org/>, accessed on 27 November 2024), and executables for different operating systems are distributed via anaconda (<https://anaconda.org/stcorp>, accessed on 27 November 2024). Within the QDOAS module of the FRM4DOAS processing, QDOAS is invoked via the command line capability and configuration files are supplied in XML (Extensible Markup Language) format.

QDOAS has been modified to directly process FRM4DOAS level-1 netCDF4 calibrated spectra files and to produce output files in netCDF4 format.

While most of the configuration files are set according to Tables 3 and 4 (see Sections 2.2.1 and 2.2.2) for the various retrieval windows used in the visible and UV wavelength regions for tropospheric and stratospheric processing, each instrument has its own set of configuration files, accounting for specific instrument features. Hence, in the framework of configuration files, as introduced in Section 2.3.2, all QDOAS configuration files are instrument-specific. Configuration files are chosen according to the instrument number and instrument channel number, extracted from the initial level-1 file name.

During the quality check of the QDOAS files (3a.1 and 3b.1 in Figure 6), it is checked whether there are any valid measurements, whether all expected gas dSCDs are present in their respective retrieval windows, and several attributes needed for further processing, as well as attributes from the level-1 file, are added.

#### 2.3.5. The Total Ozone VCD Processing Module

The module for the total O<sub>3</sub> vertical column density calculation (see Section 2.2.2 for a brief summary of the algorithm) ingests directly the QDOAS.QAQC netCDF4 files and the Level-1.QAQC files, the latter for the station location only. The original module (written in Fortran and Matlab) was re-implemented in Python. The lookup tables (LUTs)

having albedos at 380 nm and 494 nm [46], effective horizontal light paths at 500 nm, ozone airmass factor (AMF), column averaging kernel (AVK), and concentration profiles based on the TOMS v8.0 climatology [47] coupled to temperature profiles from [48] have been reformatted and saved as self-describing netCDF4 files.

Information about which O<sub>3</sub> dSCDs from which retrieval window to use is encoded as metadata in the intermediate QDOAS.QAQC files; hence, all configuration files for this module are general module configuration files; no instrument channel-specific configuration files are used.

In the QAQC for this module, one checks that the O<sub>3</sub> VCD is within the range (100–700) DU and that the relative dSCD RMS is below 10%. A relative dSCD RMS between (5–10)% is flagged as a warning in the master level-2 files and is included in the GEOMS hdf4 file.

### 2.3.6. The Stratospheric NO<sub>2</sub> Profiling Module

The module for the stratospheric NO<sub>2</sub> profiling ingests directly the QDOAS.QAQC netCDF4 files and the level-1 QAQC files, the latter for the station location information only. As for ozone, the original algorithm written in Matlab and briefly described in Section 2.2.2 (see [12] for more details) was re-implemented in Python version 3.9. The LUTs were reformatted and saved as self-describing netCDF4 files.

While the height grid, the systematic NO<sub>2</sub> error fraction and the limits for the used solar zenith angles are the same for all stations and hence are set in the module configuration file, the percentage of the a priori to create the Sa matrix, the assumed Sm covariance error (see Section 2.2.2) and the Sa residual fraction are instrument specific and hence are extracted from module-specific configuration files. Additionally, for the temperature correction, temperature information, either from the level-1 files (if provided) or from a climatology (see Section 2.3.7 for more details on the climatology), is used.

In the quality check for this module, retrievals with a low or very high degree of freedom (smaller than 0.5 or larger than 3) are flagged as invalid. Note that values between 0.5 and 1 as well as values between 2.6 and 3 are flagged as a warning in the master netCDF4 level-2 files but are included in the GEOMS hdf4 files. Measurements that have a relative RMS of measured-simulated dSCDs larger than 40% are flagged as invalid, while a relative RMS between (20–40)% is flagged as a warning. Additionally, profiles that show a double peak are flagged as invalid. Invalid values are not saved in the GEOMS HDF4 files.

### 2.3.7. The Tropospheric Profiling Module

As outlined in Section 2.2.1, FRM4DOAS currently implements the MMF [21] and the MAPA [23] tropospheric trace gas retrieval algorithms. Both ingest differential slant column densities with respect to a reference at the scan zenith. While the QDOAS analysis for HCHO already uses the scan zenith as a reference, this is not the case for NO<sub>2</sub> and O<sub>4</sub>, for which a pre-processing step is necessary. Based on the information about the scan number of each measurement and the zenith measurements before and after each scan (as identified in the level-1 QAQC processing), the measurements are re-ordered into elevation scans, and a time-averaged contribution, using the zenith before and the zenith after, is subtracted from each off-axis measurement of the scan.

Further, using the RMS between a 4-degree polynomial fit through 5 consecutive zenith measurements, an additional error on the differential slant column is calculated for those species that do not use the scan measurement as a reference in the QDOAS analysis. This extra error was introduced to account for fast time variability in the trace gas concentration.

It is possible to specify a list of elevation angles, or azimuth-elevation angle pairs, in the station-specific configuration files (see Section 2.3.4), to exclude specific elevation angles (for all azimuth directions, for specific azimuth directions or all elevation angles below a certain elevation angle) from the processing. Currently, as default, all elevation angles below 0.8° are excluded for all stations.

Both currently implemented retrieval codes need a temperature and pressure profile for the aerosol inversion. These profiles are either taken from a climatology as briefly

mentioned in Section 2.3.6 or taken from profiles provided in the level-1 file. The climatology profiles are based on data from 20 years (1995–2016) of global reanalysis by the European Centre for Medium-Range Weather Forecasts (ECMWF). Daily median values were prepared by MPIC on a global grid with a  $1^\circ \times 1^\circ$  resolution on 60 pressure levels. Within FRM4DOAS, a separate file is prepared for each station. If the level-1 file contains surface values for temperature and pressure but no profile information, the temperature profile of the lowest 5 km above surface is calculated with a fixed lapse rate of  $-6.5$  K/km.

Once this pre-processing is performed, the data are passed to the different tropospheric profiling codes via a set of dictionaries and returned as an output dictionary. Hence, new or updated codes can be connected easily.

Although both codes have their individual flagging procedure, an additional quality step is performed on the results from both codes. This is introduced since only results from the MMF retrieval code are delivered in the GEOMS files. However, MAPA results are used as an additional quality flag: The integrated partial column up to 2 km and up to 4 km is calculated and checked for consistency between both codes within their delivered uncertainties. Furthermore, it is required that at least one of the codes individually judges a scan as valid. A previous version of the processor (version 1.0) used an additional flag based on the extra error calculated from consecutive zenith measurements, see description above. Specifically, the system flagged measurement scans as invalid if the calculated extra error was larger than a factor of 3 than the median of the QDOAS estimated error of the zenith before and zenith after scans. While this does filter out conditions for which the assumption of temporal homogeneity breaks down, it also introduces a low bias on average.

To illustrate this point, we show in Figure 9 the annual variation of TROPOMI and ground-based tropospheric  $\text{NO}_2$  column measurements for Xianghe, derived from roughly 3 years of measurements (July 2019 to September 2022). We consider all valid ground-based measurements within  $\pm 1$  h of TROPOMI overpass time and calculate the corresponding daily median values. Next, we select only those days in the monthly mean that have a valid TROPOMI pixel over the measurement site as well as a valid ground-based measurement. Hence, the ground-based flagging also impacts the median values of the satellite data in the annual variation. It is clearly visible that including the extra-error flag removes days with higher concentration and hence introduces a bias in the median. Details on the TROPOMI processing version are given in Section 3.4.

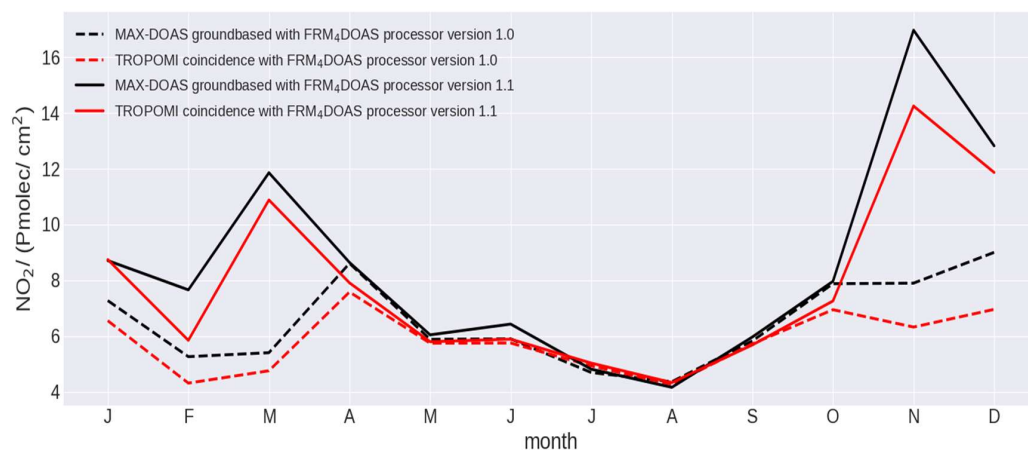


**Figure 9.** Annual variation of the tropospheric  $\text{NO}_2$  column for ground-based MAX-DOAS and TROPOMI over Xianghe, using only coincident measurements. Black curves show the ground-based median, red curves show TROPOMI median, dashed lines show the filtering with processor version 1.0, solid lines with filtering of processor version 1.1. For details, see text.

For the OEM-based retrieval code (MMF), the standard a priori profiles correspond to decreasing exponential profiles with a scale height of 1 km, and the default integrated column up to 4 km is  $9 \times 10^{15}$  molec/cm<sup>2</sup> for  $\text{NO}_2$  and  $8 \times 10^{15}$  molec/cm<sup>2</sup> for HCHO. If

one year of data are available at a station, suitable adjustments for each station are made for the integrated a priori value based on the mean from the geometric approximation of at least one year of data. Likewise, the covariance matrix for MMF is constructed from the a priori profiles (50% on the diagonal, 200 m correlation length for calculating the off-diagonal elements).

Since MAPA uses pre-calculated LUTs in combination with a parameterisation approach, no a priori values are needed. However, since, e.g., the surface albedo is currently not a parameter, stations located in areas for which the surface albedo greatly deviates from the standard value of 0.06 (that was used for the LUT creation) should be handled with caution. Additional LUTs for different conditions are currently prepared by MPIC to overcome this limitation.

Apart from the profiling of trace gases and aerosols, the tropospheric processing module currently implements the broken clouds algorithm of Gielen et al. [42] and the effective distance calculation developed in the framework of the EU FP7 QA4ECV project [49]. However, the broken cloud flag is currently not used since the implementation will soon change to the algorithm described in Section 2.2.3.

### 2.3.8. Delivery to NDACC and EVDC Databases and Processing Status

At the time of writing, only total ozone VCD level-2 GEOMS HDF4 and tropospheric NO<sub>2</sub> (from UV channel) profile level-2 GEOMS HDF4 files are submitted to the NDACC database. As with any other module, this task is also handled via a trigger list and a dedicated wrapper. The processes are graphically outlined in Figure 10. As for other modules, whether a file name is listed and handled via configuration files depends on the module and the instrument in question.

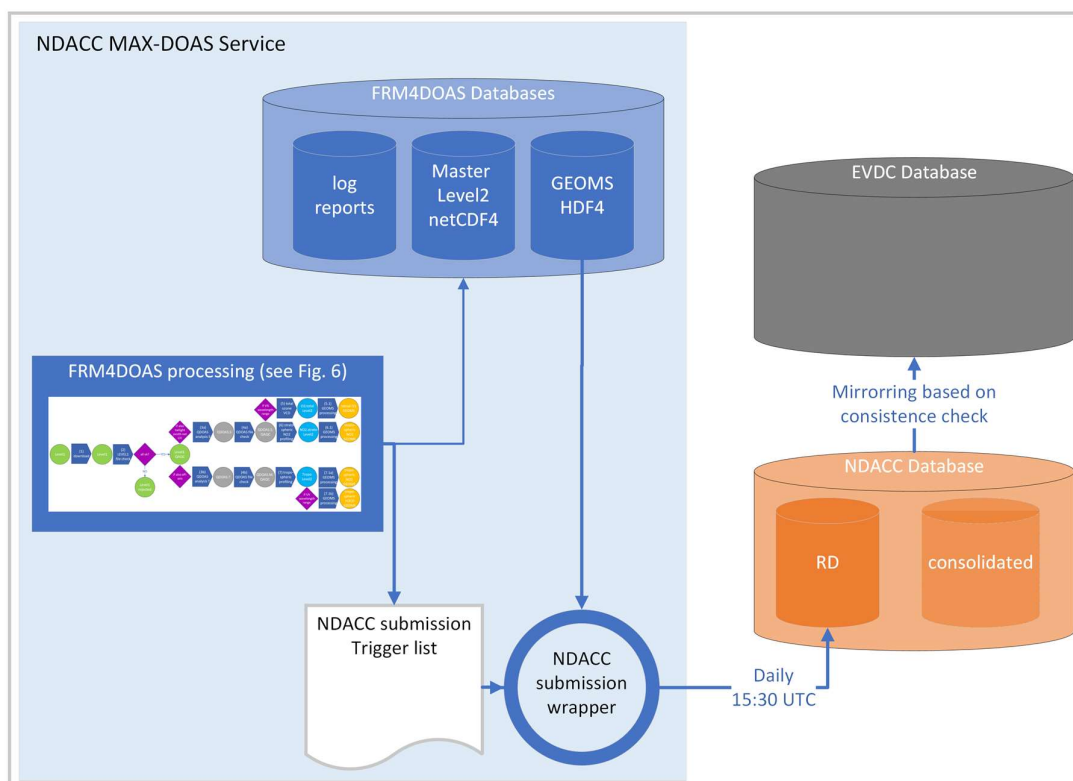


**Figure 10.** Current workflow for the submission to NDACC and EVDC databases.

As indicated in Figure 10, submission happens once per day at 15:30 UTC. Before being catalogued in the NDACC rapid delivery repository (RD, <ftp://ftp.cpc.ncep.noaa.gov/ndacc/RD/>, accessed on 27 November 2024), the files must pass the NDACC QA/QC check. Further submission to EVDC is performed via a mirroring approach.

### 2.3.9. System Sustainability and Long-Term Stability of the Products

The FRM4DOAS system is not a network on its own but a service attached to the NDACC network and to the ACTRIS European Research Infrastructure. The long-term operation of the system therefore depends on the sustainability of these entities and on the ability of the station PIs to gain the necessary funding for operating their instruments. However, the central processing system can provide support to data providers in light of ensuring the long-term stability of the generated data products. This goes through the implementation of automated monitoring tools and reporting systems (e.g., checks on fitting RMS, spectral shift, automated horizon scans, etc.) and through the establishment of Standard Operation Procedures (SOPs) providing guidance to PIs to check and report on the maintenance of their instruments. It also goes without saying that in order to expand and continue the service, we rely on continued funding for (a) code maintenance and evolution, (b) file storage and (c) computational costs.

## 3. Results

In this section, we describe the work performed to validate and assess the performance of the FRM4DOAS processing system, and we provide examples of its application to support campaign activities and for satellite validation.

### 3.1. FRM4DOAS Validation and Performance Assessment

Validation of the processing system is complex and covers many different aspects, including validation of technical aspects such as the timelines of the processing of data, consistency in formats, feedback to users and proper reactions to error situations. These more technical points will not be covered here.

A rigorous validation of the profiles retrieved by the system would consist of comparisons with independent profile information. Such a validation exercise is a major task and is limited by the availability of reference data. The approach taken here was therefore to apply the processing system to data from a subset of instruments operating during the CINDI-2 campaign [10], to evaluate the data for consistency, plausibility and coverage, and to compare the results to the validation data available from the campaign. This part is based on work performed in the framework of the CINDI-2 profile intercomparison exercise published in [50].

The subset of instruments used for the results of the CINDI-2 campaign is listed in [50] (Table 2). Instruments of different campaign performances were chosen to cover a broader range of input data quality. Instrument performances were assessed during the CINDI-2 semi-blind intercomparison exercise as described in [10]. The instrument subset for this validation includes two double-channel high signal-to-noise (SNR) scientific instruments (BIRA and IUP-Bremen), one scientific single-channel standard SNR instrument (AUTH) and one commercial two-channel Envimes/Airyx instrument (DLR/USTC). For the analysis of this dataset, the processing system was applied to the level-1 data submitted during the CINDI-2 campaign. The version of the processing system was validation\_01.0.

All four options of the processing system (the optimal estimation retrieval MMF) and three flavours of the parametric MAPA retrieval using a fixed  $O_4$  scaling factor [51] of 0.8, a fixed scaling factor of 1.0 and a fitted  $O_4$  scaling factor were included. No  $O_4$  scaling is applied in the MMF implementation.

Before validating the profile retrievals with independent data, a comparison was performed between the results from the different retrievals (MMF and MAPA with three different approaches to the  $O_4$  scaling factor). While overall, the retrievals showed good qualitative agreement, several interesting observations were made. As is often the case for retrievals based on optimal estimation, if no strong regularisation was used, there were cases where MMF retrievals found elevated layers, both for aerosols and for trace gases. In the case of aerosols, this was sometimes but not always linked to clouds at the given altitude. The differences between the two retrieval types were smaller for instruments with

a good SNR than for those with more noise, in particular for UV retrievals. On average, the MAPA retrieved a larger AOD, often at higher altitudes.

One important issue that became apparent during the comparisons was the large number of profiles flagged as invalid. Flagging between the retrievals was not consistent, and for one instrument with a lower SNR, all HCHO profiles were flagged as invalid.

During the CINDI-2 campaign, surface concentrations of  $\text{NO}_2$  and HCHO were determined with continuous LP-DOAS measurements taken in a measurement volume close to that observed by the MAX-DOAS instruments. These data can be used to validate the surface concentrations retrieved from the MAX-DOAS measurements.

In Figure 11, results are shown for both the median of the datasets and for individual data points. For HCHO, the median of the retrievals fits excellently with the LP-DOAS values throughout the campaign, regardless of weather conditions. This is surprising, as HCHO absorption is small, and HCHO profiles are usually subject to noise. Possible explanations are less vertical variability making the a priori used more representative of the real situation or less horizontal variability when compared to  $\text{NO}_2$ . Comparing individual results, MAPA 1.0 and MMF tend to be lower than the other two MAPA versions on many days. Overall, the scatter of individual results is not insignificant but mostly of the order of 30%.

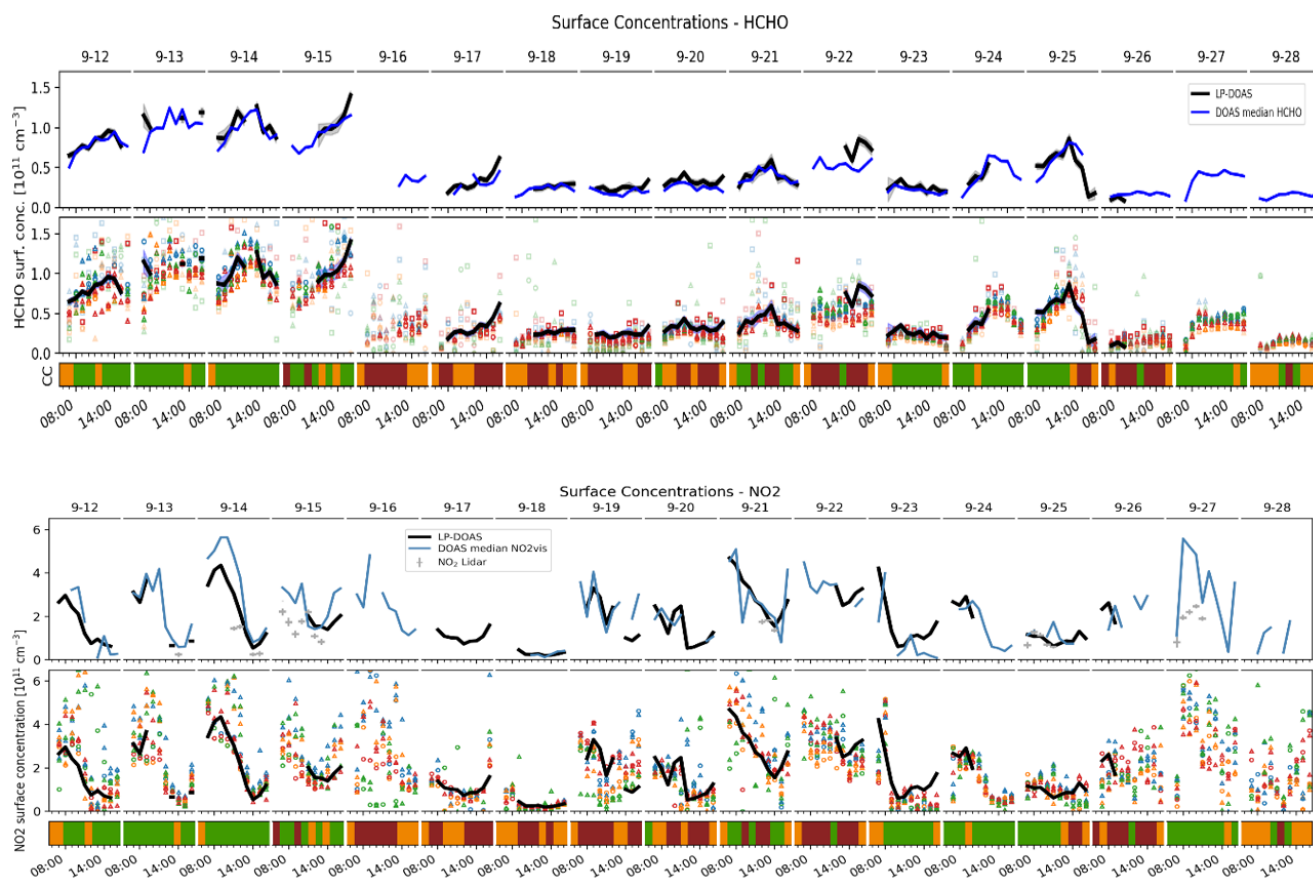


**Figure 11.** Comparison of retrieved surface concentrations of HCHO (top) and  $\text{NO}_2$  (bottom) with LP-DOAS observations during CINDI-2 (12–28 September 2016). The upper panel in each figure shows the comparison between LP-DOAS (black) and the median of the data (blue); the lower panel includes all individual values (represented in different colours). Results from invalid profiles are shown in washed-out colours. For  $\text{NO}_2$ , lidar data are included as grey crosses where available. The colorbar at the bottom of the figure specifies the cloud conditions. Green stands for good, orange for critical and red for bad conditions.

For  $\text{NO}_2$ , there is more variability, and at least on some days, there is a clear underestimation of the surface  $\text{NO}_2$  in the morning by the median of the MAX-DOAS retrievals, mainly driven by MAPA results. When looking at individual values, the scatter is large, partly more than 100%, and no clear pattern of which algorithm or instrument yields lower or higher values can be identified. The large variability is a surprise given the much stronger absorption signal when compared to HCHO, but the confinement of the  $\text{NO}_2$  to a shallow layer close to the surface makes retrieval of surface concentrations from MAX-DOAS measurements difficult. As is the case for HCHO, there is no clear indication for better results under clear-sky conditions.

In addition to surface concentrations, also vertical tropospheric columns of  $\text{NO}_2$  can be compared to independent measurements, in this case, results from direct sun observations also performed during the campaign [50]. The latter are insensitive to the vertical profile of  $\text{NO}_2$  and can therefore be considered as much more accurate than vertical columns retrieved from MAX-DOAS data. The results are shown in Figure 12. Surprisingly, there is a clear overestimation of the  $\text{NO}_2$  column by the MAX-DOAS retrievals during the first days, which could be linked to the underestimation of the surface concentrations discussed above. Compared to the surface concentrations, the scatter in the vertical columns is much reduced, indicating that the column is a better-constrained retrieval quantity than the surface concentration. This supports the hypothesis that deviations in the  $\text{NO}_2$  surface concentrations are a result of a shifting/smoothing of gas into higher layers.

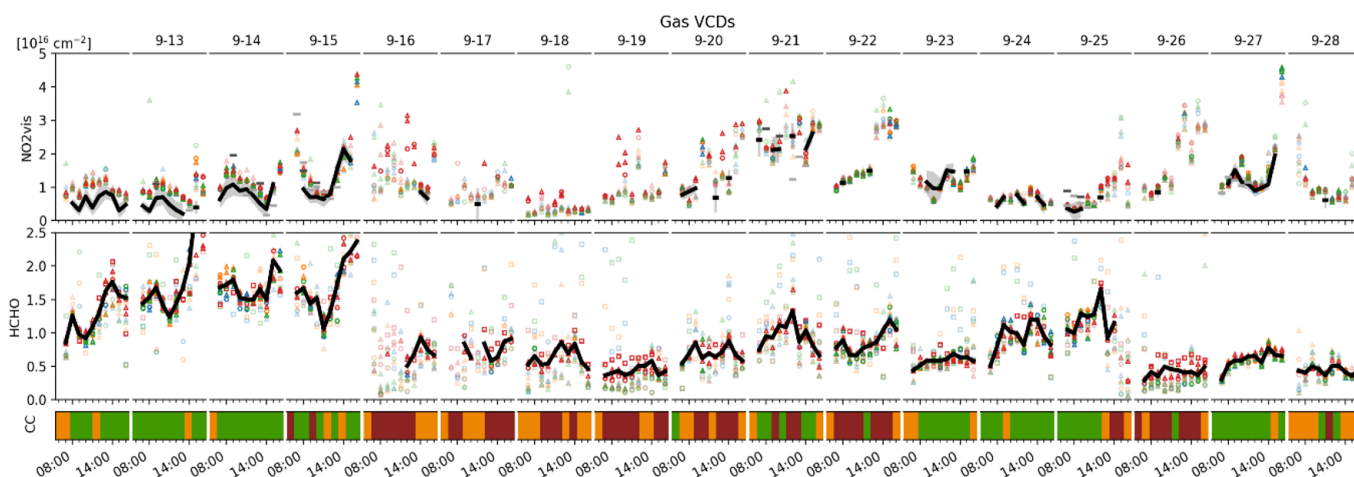


**Figure 12.** Comparison of all retrieved tropospheric columns of  $\text{NO}_2$  and results from direct sun measurements (top) and comparisons of HCHO median values with all individual retrievals (bottom). The grey-shaded area in the  $\text{NO}_2$  panel indicates the uncertainty of the direct sun columns. Other descriptions of Figure 11 apply.

Also shown in Figure 12 is a comparison between individual HCHO columns and the median values. This comparison is less instructive, but there are unfortunately no independent HCHO columns available for comparison. As for  $\text{NO}_2$ , the scatter in the columns is much less than in the surface concentrations. During the cloudy parts of the campaign, the scatter increased, but most of these retrievals are flagged as invalid.

For the aerosol retrievals, the results can be compared to AOD measurements from a CIMEL sun photometer located at the MAX-DOAS measurement site. This comparison is shown in Figure 13 for both wavelengths and two different ways to calculate the AOD, total AOD and partial AOD. The latter accounts for the fact that MAX-DOAS retrievals are sensitive only to the lowest part of the extinction profile and therefore combine the vertical extinction profile from the ceilometer with the averaging kernels of the measurements to compute that part of the sun-photometer observed AOD that is accessible to MAX-DOAS measurements. Details of this approach are given in [50].

As can be seen from Figure 13, MAX-DOAS AOD retrievals follow the temporal evolution of the sun-photometer AOD well. During the first days, agreement with the partial AOD is clearly better than with the full AOD as expected. When evaluating individual MAX-DOAS retrievals, there is a clear tendency for MMF and MAPA 1.0 retrievals to underestimate sun-photometer AODs, whereas the other two MAPA retrievals are closer to the validation data. This could be interpreted as support for the need for an  $O_4$  scaling factor as, for example, discussed in [51].

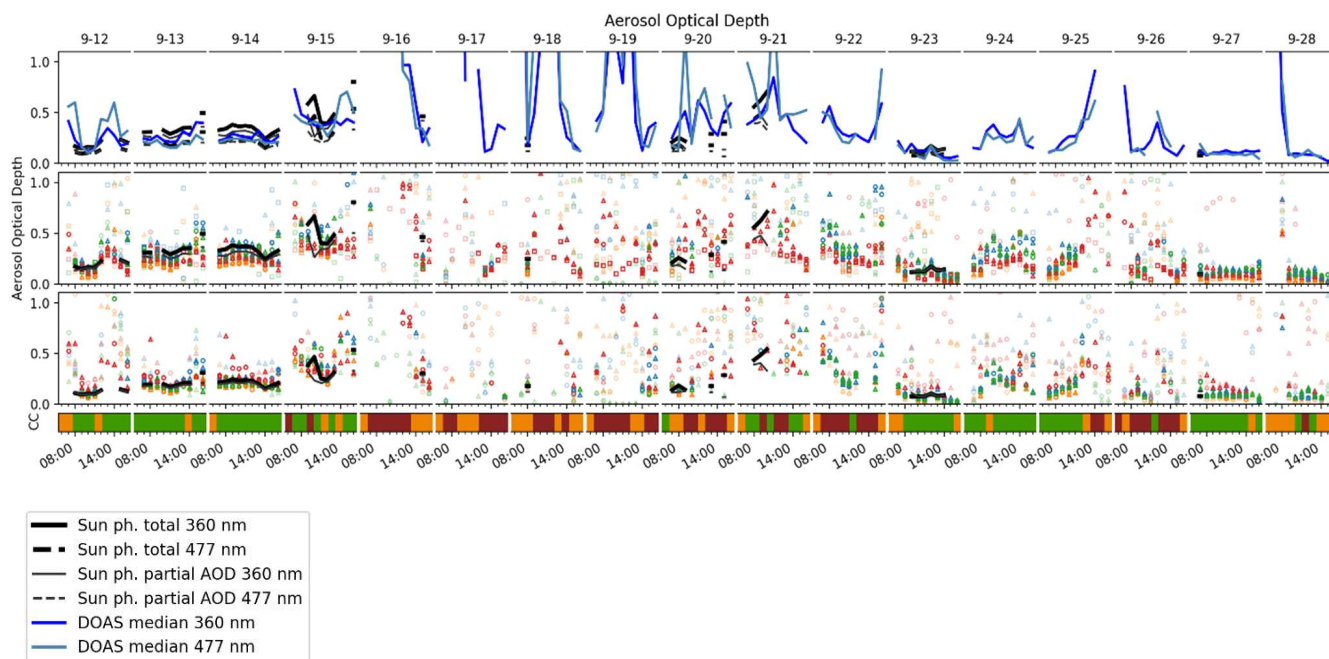


**Figure 13.** Comparison of MAX-DOAS and sun-photometer retrieved AOD during the CINDI-2 campaign (12–28 September 2016). The first row shows the comparison between medians and total and partial sun-photometer AOD; the second and third rows show all results for the UV and the vis aerosol retrievals. Other descriptions of Figure 11 apply.

As expected, AOD values vary widely during cloudy days, and no validation data are available, as sun-photometer measurements are only possible during clear-sky periods.

While the scope of this validation exercise is limited to a few days and one location, it shows the overall good performance of the FRM4DOAS system for aerosols,  $NO_2$  and HCHO retrievals. Data from instruments with different characteristics could be ingested, and results are consistent with long-path and CIMEL validation data. The deviations observed as well as the problems with some oscillating profiles, challenges when  $NO_2$  is constrained to a very shallow layer and limited sensitivity above 2 km are typical for MAX-DOAS retrievals and not specific to FRM4DOAS. The large number of retrievals flagged as being invalid is a serious problem and has therefore been addressed in more recent versions of the processor (see also Section 2.3.7).

### 3.2. NDACC Rapid Delivery Demonstration Service

As already explained in Section 2.3.8, the FRM4DOAS system delivers daily total ozone as well as tropospheric  $NO_2$  vertical profile level-2 GEOMS HDF files to the NDACC rapid delivery repository. Tropospheric formaldehyde and stratospheric  $NO_2$  vertical profiles are not distributed yet, but they are processed together with the other products and internally monitored.

The submission to the NDACC happens once per day at 15:30 UTC, and once catalogued on the NDACC, the data are further deposited on the ESA EVDC database by mirroring. The service started in December 2020 and, since then, has been operated without



interruption. Most stations deliver data at a daily frequency, and where possible, the processing of the data has been extended back to July 2018, which corresponds to the official start of the demonstrational Central Data Processing System. At some stations, historical datasets are available back to early 2000. A full reprocessing of these data is among the planned activities when moving the system into a fully operational status.

Table 9 provides an overview of the distribution of the retrieved data products at the different stations of the network. The product availability is mostly driven by instrument specifications, in particular the geometry of observation and the spectral range covered by the spectrometers available at the different sites. High-altitude sites are currently excluded from tropospheric NO<sub>2</sub> and HCHO processing due to the low concentration of these molecules at free-tropospheric altitudes, and the difficulty to interpret such measurements for satellite validation.

**Table 9.** Distribution of the data products generated by the FRM4DOAS Central Data Processing System. Total ozone and tropospheric NO<sub>2</sub> vertical profile data that are submitted daily to the NDACC rapid delivery (RD) repository are denoted by filled circles. Other products generated by the system but not submitted to the NDACC RD are denoted by open circles.

Station	Institute	Total O <sub>3</sub>	Tropo NO <sub>2</sub>	Tropo HCHO	Strato NO <sub>2</sub>
Ny-Alesund	IUP Bremen	●	○	○	
Harestua	BIRA-IASB	●			○
Bremen	IUP Bremen	●	●	○	○
De Bilt	KNMI	●	●	○	○
Cabauw	KNMI		●	○	○
Uccle	BIRA-IASB	●	●	○	○
Vielsalm	BIRA-IASB		○	○	○
Mainz	MPIC		●	○	○
Heidelberg	IUP Heidelberg	●	●	○	○
Jungfraujoch	BIRA-IASB	○			○
San Pietro Capofiume	CNR-ISAC	○	○	○	○
Toronto Downsvie	ECCC		○	○	○
Thessaloniki	AUTH-LAP	●	●	○	○
Xianghe	BIRA-IASB	●	●	○	
Athens	IUP Bremen	●	●	○	○
Izana	INTA	●			○
Kinshasa	BIRA-IASB		○	○	
La Reunion Mairo	BIRA-IASB	●			○
Lauder	NIWA	●	●	○	○
Neumayer	IUP Heidelberg	●	○	○	○
Utsteinen	BIRA-IASB	○	○	○	○
Arrival Heights	IUP Heidelberg	●	○	○	○

Figures 14 and 15 give a visual overview of the status of the data processing for tropospheric NO<sub>2</sub> vertical profiles and for total ozone, respectively. Note that for double-channel instruments (i.e., those for which the UV and visible channels are reported in different files), we produce NO<sub>2</sub> GEOMS files both for the UV and for the visible channels. However, for those instruments that are part of the NDACC service (see Table 9), only the visible is submitted to the RD repository unless there is no visible channel at all.

Due to limited resources, the FRM4DOAS system has so far been operated in a demonstrational mode, with an emphasis on rapid data delivery to the NDACC and ESA's EVDC data centres. In a subsequent step of the project, it is planned to extend the processing to historical data series available at the different stations listed in Table 9. Among them, 15 sites have time series extending over more than 10 years, and 7 feature data series covering more than 20 years of measurements. Such data records will expand the capabilities of the NDACC network to address long-term variability and trend studies as well as the validation of historical satellite data records.

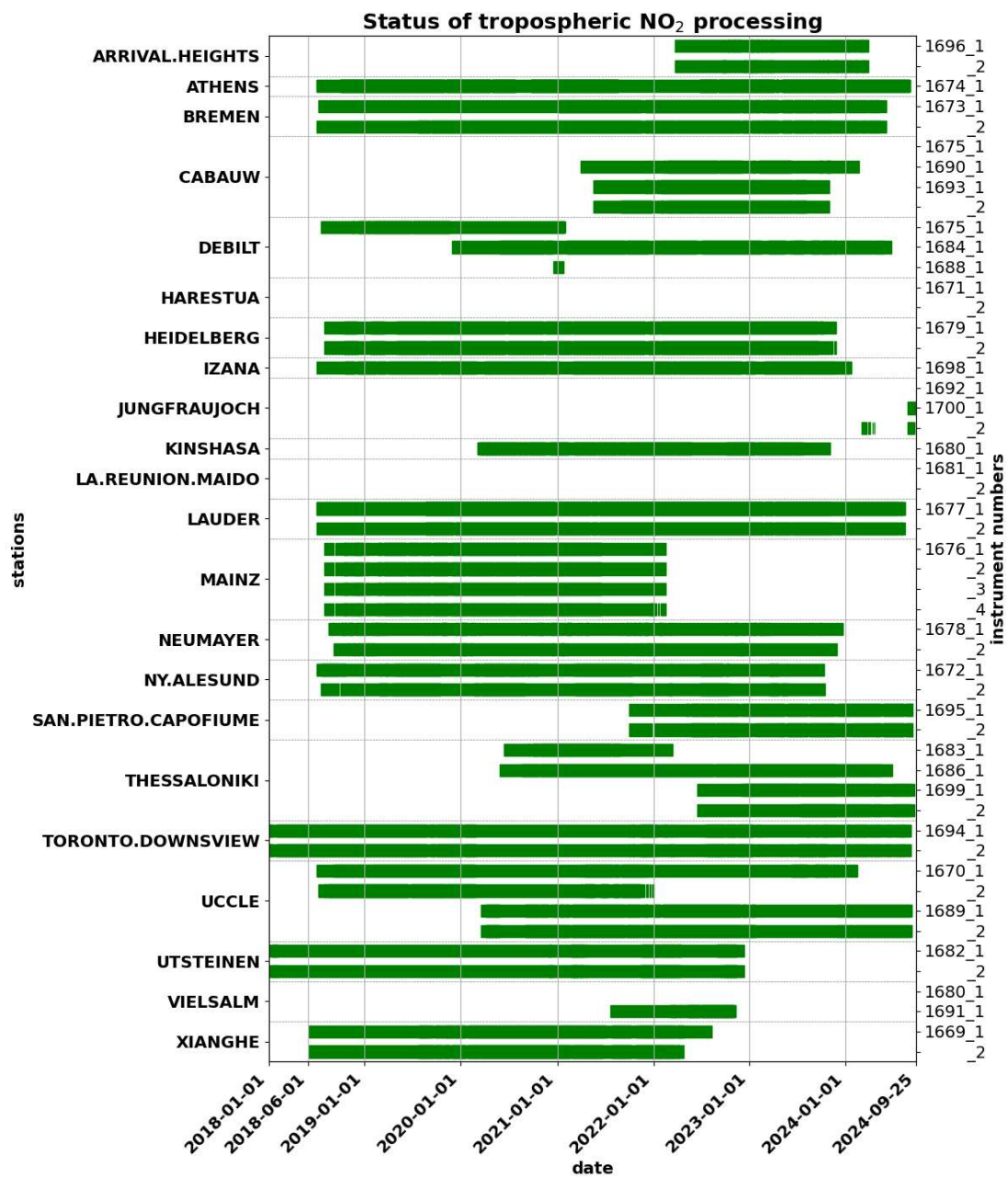


Figure 14. Overview of the FRM4DOAS tropospheric NO<sub>2</sub> vertical profile demonstrational data processing covering the period from January 2018 until late September 2024. Note that for double-channel instruments, NO<sub>2</sub> files are produced both for the UV and visible channels.

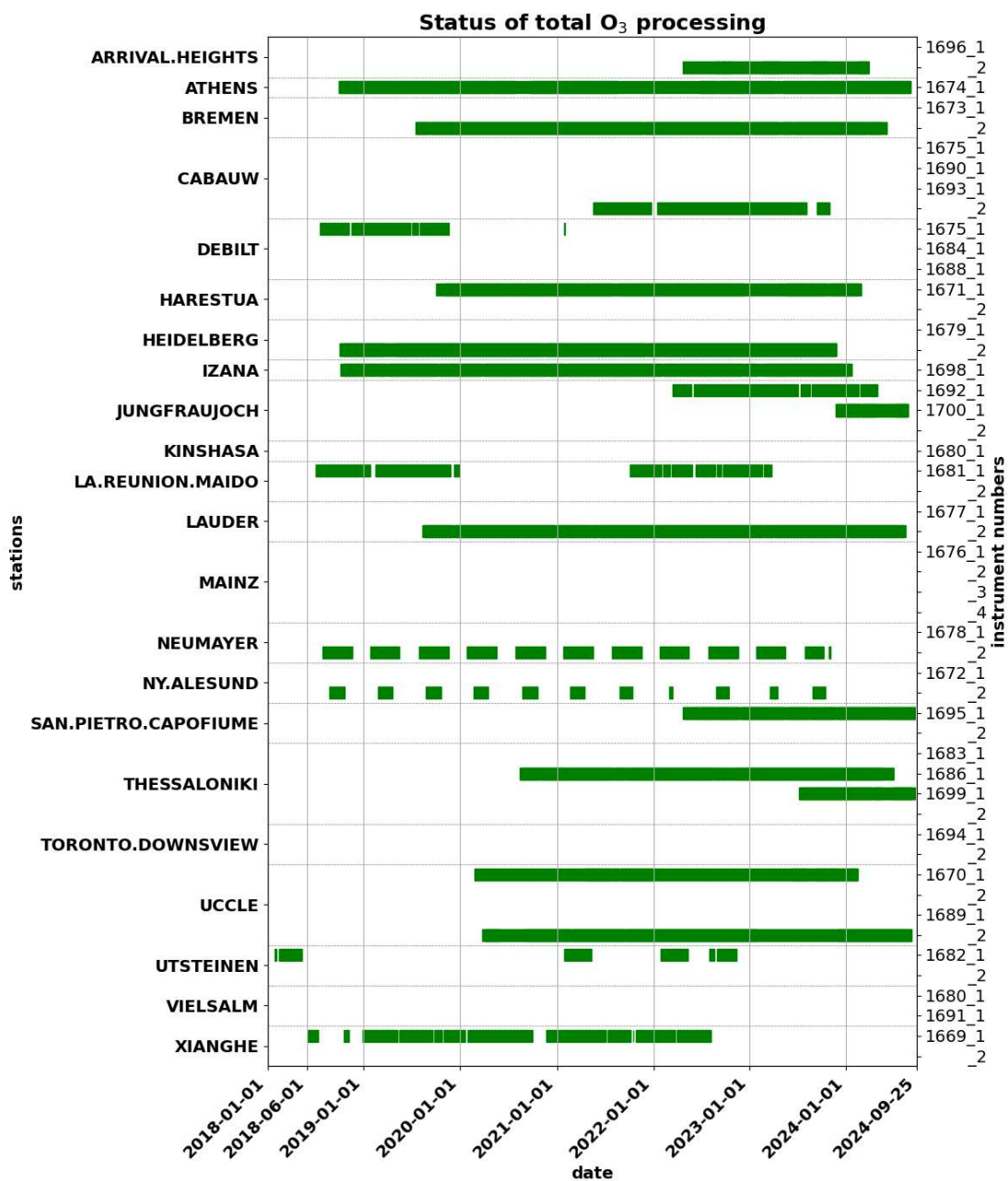


Figure 15. Overview of the FRM4DOAS total ozone demonstrational data processing covering the period from January 2018 until late September 2024.

### 3.3. Field Campaign Support

In addition to processing data from static stations, FRM4DOAS was also used in support of a number of international field campaigns. A list of these campaigns, that took place between 2016 and 2022, is given in Table 10. They generally involved both MAX-DOAS and PANDORA systems as well as airborne imaging DOAS instruments, and their focus was on air quality characterisation using remote-sensing techniques as well as satellite validation.

Figure 16 illustrates the results from the application of the FRM4DOAS system to ground-based measurements during the GMAP campaign. This campaign took place in the Republic of South Korea in October and November 2021 and aimed to validate the GEMS (Geostationary Environmental Monitoring Spectrometer) instrument on board the GEO-KOMPSAT-2B platform that was launched a few months earlier. In early October, several instruments were collocated in Incheon city before being deployed inside and

around the Seoul metropolitan area. The figure shows results from the intercomparison of NO<sub>2</sub> and HCHO VCD measurements from three collocated instruments in Incheon: the IUP Bremen research grade MAX-DOAS, an Airyx Skyspec operated by BIRA and a PANDORA operated by the Pukyong National University (PKNU). All measurements were filtered according to the approach described in Section 2.3.7.

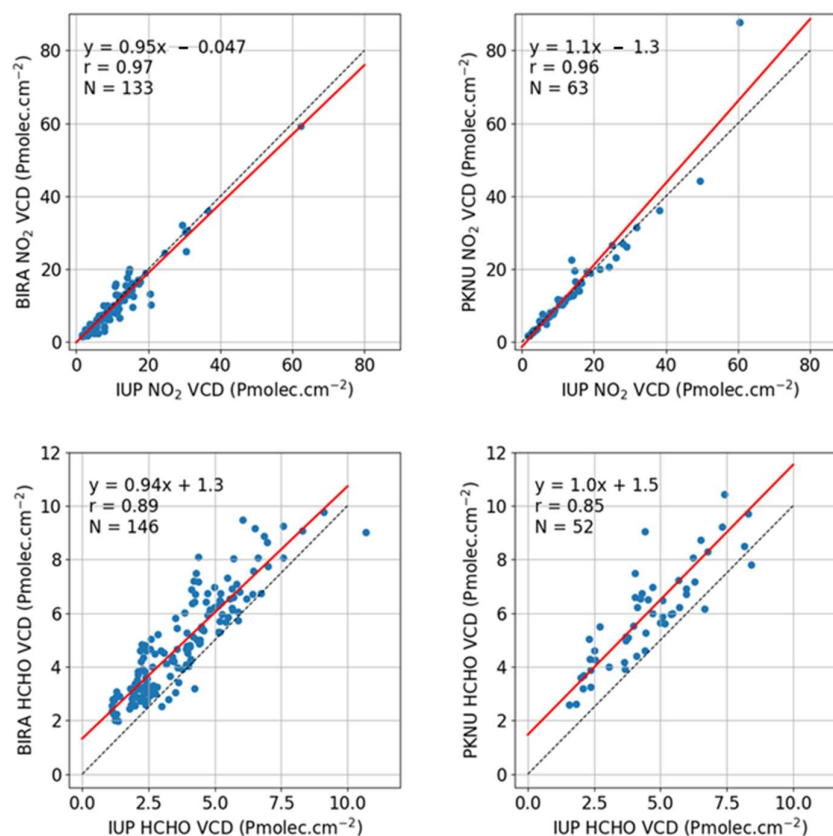


**Figure 16.** Intercomparison of NO<sub>2</sub> and HCHO VCD from three collocated instruments during the GMAP 2021 campaign (Incheon, South Korea, October 2021). The red shows the linear regression line, while the dashed black line corresponds to the 1:1 line.

From inspection of Figure 16, one concludes that all three systems agree well for NO<sub>2</sub> VCD (upper panels) with a slope and a Pearson correlation coefficient both close to unity. The level of agreement slightly degrades for HCHO, but it remains acceptable considering the weaker sensitivity of the measurement technique to this molecule. Overall, this demonstrates the good level of consistency achievable in a campaign between different instruments (of different designs) when these are centrally processed using FRM4DOAS.

**Table 10.** International field campaigns involving FRM4DOAS. For each campaign, the number of instruments that were processed using the FRM4DOAS system is indicated.

Campaign Acronym	Campaign Objective	Location	Date	Number of Instruments	Reference
CINDI-2	Intercalibration of UV–Visible trace gas remote sensing instruments	Cabauw, Netherlands	September 2016	15	[50]
TROLIX	Geophysical validation of Sentinel-5p/TROPOMI data products using the Dutch Ruisdael Observatory	Cabauw, Netherlands	September–October 2019	6	[52]

Table 10. Cont.

Campaign Acronym	Campaign Objective	Location	Date	Number of Instruments	Reference
QA4EO	Validation of Sentinel-5p/TROPOMI NO <sub>2</sub> product using airborne and ground-based measurements	Ruhr, Germany	August–September 2021	1	[53]
GMAP-2020	First validation campaign of the GEO-KOMPSAT-2B GEMS instrument	Seoul, South Korea	October–November 2021	5	[54]
SIJAQ-2022	First validation campaign of the GEO-KOMPSAT-2B GEMS instrument	Seoul, South Korea	June–August 2022	6	[55]

### 3.4. Application to Sentinel-5 Precursor and GEMS Validation

The FRM4DOAS datasets have been used for the validation of tropospheric NO<sub>2</sub> and HCHO satellite datasets, including GOME-2 [56], S5p/TROPOMI [57] and GEMS. The HCHO datasets have also been used for model evaluation [58], and the NO<sub>2</sub> and HCHO data from the Kinshasa site have been studied in detail in [59].

An overview of the TROPOMI tropospheric NO<sub>2</sub> validation results using the FRM4DOAS sites is given in Figures 17 and 18. Following the approach described in [57], only TROPOMI pixels containing the site are compared to the MAX-DOAS data. TROPOMI data are from the latest version of the operational processor (RPRO v2.4 and OFFL ≥ 2.4, see [60]) and the MAX-DOAS data are all based on the FRM4DOAS processing.

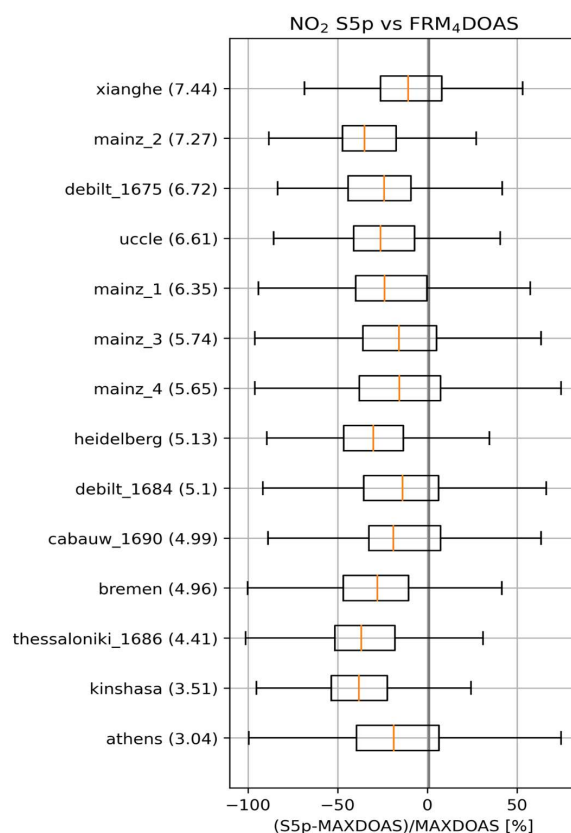


**Figure 17.** Box-and-wisher plot of the daily relative biases for S5p/TROPOMI tropospheric NO<sub>2</sub> v2.4 vs. MAX-DOAS from the FRM4DOAS processing chain main stations (mid-July 2018 to December 2023). The stations are ordered from bottom to top by increasing median NO<sub>2</sub> MAX-DOAS VCD values (values given in brackets in units of 10<sup>15</sup> molec.cm<sup>-2</sup>).

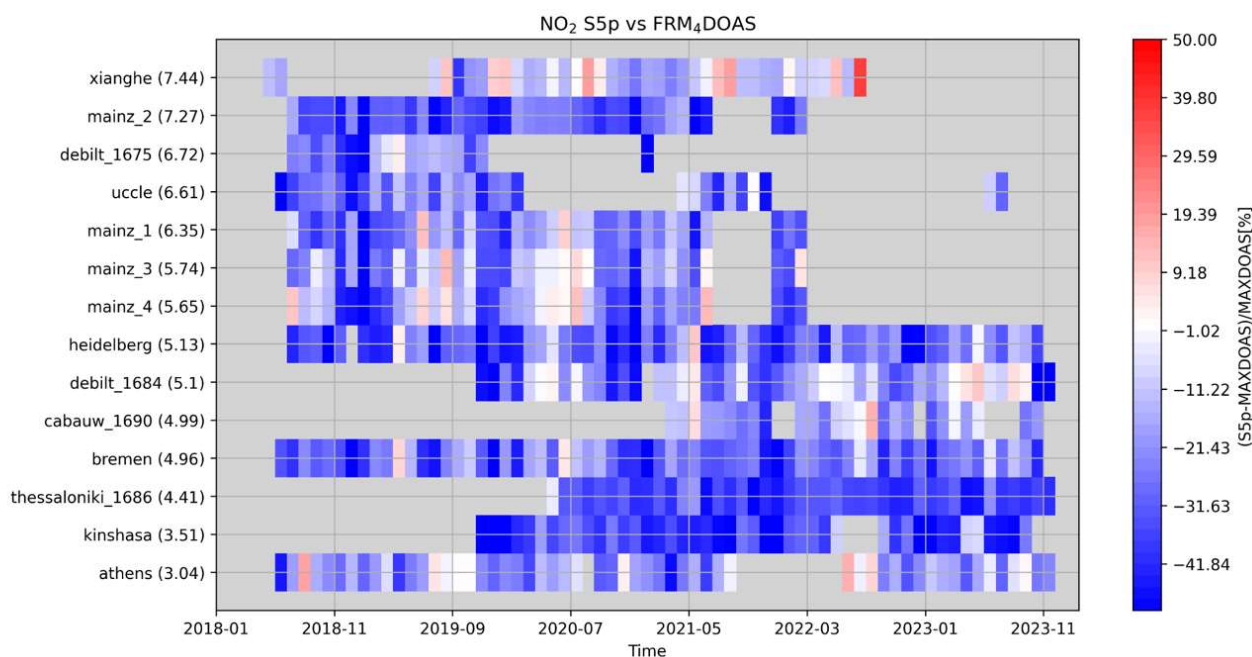


**Figure 18.** Mosaic plot of the monthly median relative biases for S5p tropospheric NO<sub>2</sub> v2.4 vs. MAX-DOAS based on the FRM4DOAS processing. As in Figure 17, the stations are ordered from bottom to top by increasing median NO<sub>2</sub> MAX-DOAS VCD values (values given in brackets in units of 10<sup>15</sup> molec.cm<sup>-2</sup>).

In line with previous validation results (e.g., [57]), a systematic negative bias is observed in TROPOMI data at all sites, with values ranging between  $-11\%$  at Xianghe and  $-38\%$  at Kinshasa. It was shown in the literature that this negative bias can be reduced when the MAX-DOAS profiles and the TROPOMI vertical sensitivity are considered, see e.g., [16,59]. Depending on the MAX-DOAS viewing direction (see results for Mainz in Figure 17), the bias can vary from around  $-15\%$  (Mainz\_4 and Mainz\_3) to  $-24\%$  (Mainz\_1) and up to  $-35\%$  (Mainz\_2) in the most polluted viewing direction. Advanced comparison techniques considering the MAX-DOAS field-of-view direction and the wavelength dependency of the NO<sub>2</sub> absorption can also be used to better consider the impact of horizontal inhomogeneities [16]. In the present case, the network median relative bias is  $-24\%$  ( $-1.32 \times 10^{15}$  molec/cm<sup>2</sup> in absolute), with a dispersion (IP68/2) of the station medians of  $9.5\%$  ( $3.99 \times 10^{14}$ ) and a spread (median of the stations' dispersions) of  $27\%$  ( $2.3 \times 10^{15}$ ).

TROPOMI NO<sub>2</sub> validation has been regularly performed within the ATM-MPC ESA project, relying on quarterly updates of validation reports (e.g., ROCVR 22, available on <https://s5p-mpc-vdaf.aeronomie.be/>, accessed on 27 November 2024) and operational comparisons performed by the automated validation server AVS (<https://mpc-vdaf-server.tropomi.eu/>, accessed on 27 November 2024). Both include comparisons with MAX-DOAS data, provided by each MAX-DOAS Principal Investigator (PI) to BIRA-IASB in the first case (through the NIDFORVAL project, N4V [57]), uploaded on the NDACC rapid delivery database and mirrored by EVDC in the second case. Figure 19 presents an overview of the validation results for the three treatments, focusing on the stations of Athens, Bremen, Cabauw, De Bilt, Kinshasa, Mainz, Uccle and Xianghe. One can see that for these stations, the results of the three treatments are consistent with each other although different choices were made in implementing the comparison (e.g., interpolation or averaging of the ground-based data, use of the station coordinates or the ground-based data air-masses location for the satellite pixel selection). An interesting feature is the reduction in the comparison spread when moving from individually processed MAX-DOAS data (as for N4V and AVS cases) to the harmonised FRM4DOAS system. Once fully operational, the FRM4DOAS data stream will become the reference data stream for the S5p validation.

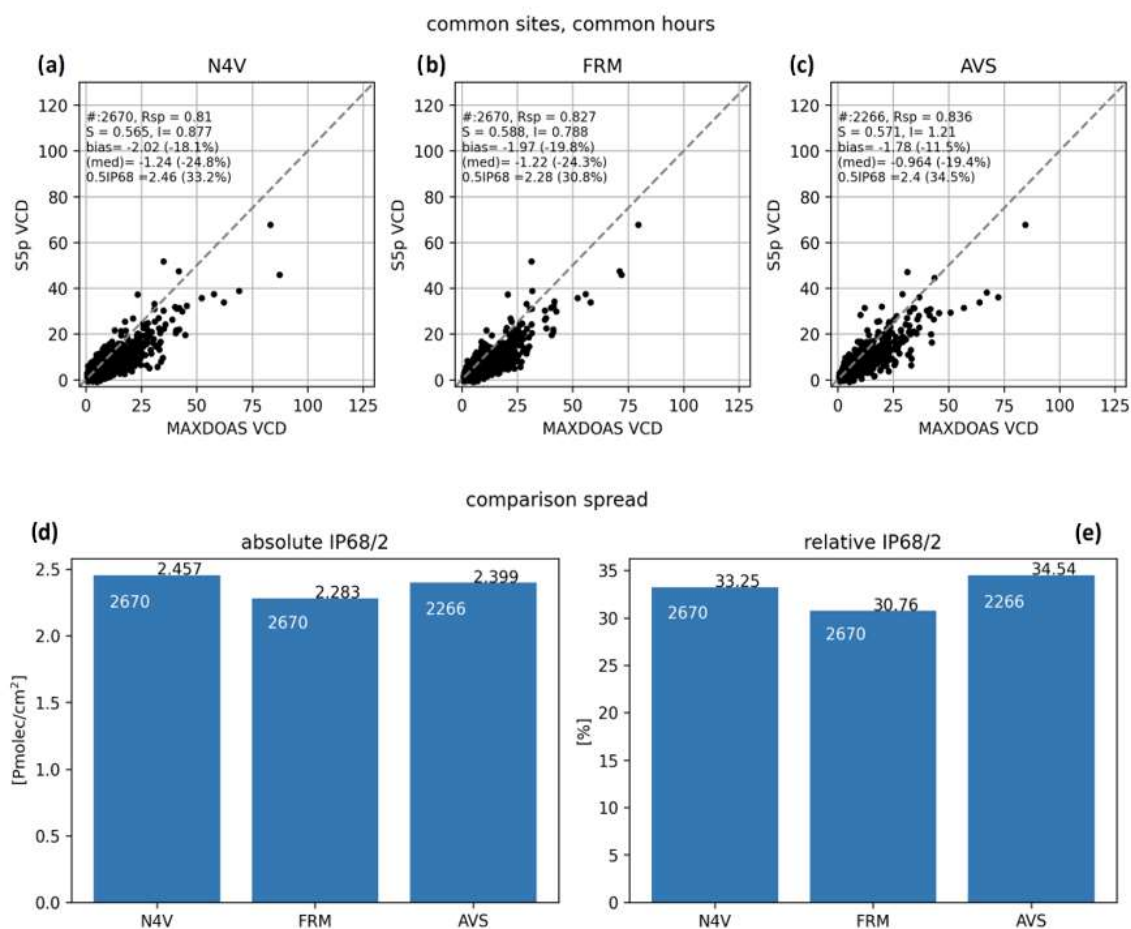


**Figure 19.** Overview plot of the S5p tropospheric NO<sub>2</sub> v2.4 vs. MAX-DOAS comparisons results based on the NIDFORVAL (N4V), FRM4DOAS (FRM) and automated validation server (AVS) treatments for a subset of sites (see text). Panels (a–c) present scatter plots for each case including statistics information, and panels (d,e) summarise the final comparison spread in absolute and relative cases as bar plots.

As discussed in Section 3.3, NO<sub>2</sub> and HCHO data from the GMAP21 and SIJAQ22 campaigns were processed using the FRM4DOAS centralised facility. These datasets have been used for the validation of GEMS together with data from stationary instruments operated in Xianghe, Mohali, Yokosuka, Chiba and Kasuga, the latter stations being processed using their own non-harmonised retrievals [61–63]. This allowed for expansion of the validation of GEMS HCHO data, which until then was relying on a limited number of ground-based data [64]. More detailed comparisons during the GMAP 2021 and SIJAQ 2022 campaigns can be found in [54] and in [55] for HCHO and NO<sub>2</sub>, respectively, using both (FRM4DOAS) MAX-DOAS and Pandora instruments and focusing on GEMS and TROPOMI satellite data.

#### 4. CEOS FRM Self-Assessment

The CEOS Working Group Cal/Val (WGCV) recently developed a tool to enable Cal/Val data providers to evaluate to what extent they are CEOS-FRM compliant and, if not, to report on their intended progress towards reaching full compliance. CEOS-Fiducial Reference Measurements are defined as “*independent, fully characterised, and traceable measurements, tailored specifically to address the calibration/validation needs of satellite borne instruments making measurements of a particular measurand, that follow the guidelines outlined by the GEO/CEOS Quality Assurance framework for Earth Observation (QA4EO)*” [65]. In practice, the evaluation framework takes a pragmatic approach relying on a self-assessment of the

status of the FRM against a set of criteria that are subject to peer review through a board of experts led by CEOS WGCV. The degree of compliance with those criteria is based on a gradation scaling rather than a simple fail/pass approach. The outcome of the evaluation is presented in the Maturity Matrix model [65], which provides a simple visual assessment of the state of the CEOS-FRM for all given criteria, making visible where it is mature and where evolution and effort are needed.

Table 11 shows the Maturity Matrix for the FRM4DOAS system obtained by self-assessment following the guidelines proposed by the CEOS WGCV. Several categories are graded as Ideal or Excellent, including the Operator Expertise, Automation Level, Availability and Data Format. Most of the other categories are graded as Good, except for “Utilisation/feedback” and “Independent verification”, which are currently graded as Basic. The low level of assessment for these two criteria is largely due to the current demonstrational status of the service, which limits its usage and verification. We anticipate significant progress on these criteria from 2025, when FRM4DOAS will enter an operational phase, and a greater number of users and applications will be served by the system.

**Table 11.** Self-established Maturity Matrix for the FRM4DOAS service. The meaning of the colours is defined in Table 12 and follows the CEOS-FRM standards.

Nature of FRM	Self-Assessment				
	FRM Instrumentation	Operations/Sampling	Data	Metrology	Verification
Descriptor	Operator expertise	Automation level	Data completeness	Uncertainty characterisation	Guidelines adherence
Range of instruments	Instrument documentation	Measurand sampling/representativeness	Availability and usability	Traceability documentation	Utilisation/feedback
Complementary observations	Evidence of traceable calibration	ATBD on processing/software	Data format	Comparison/calibration of FRM	Metrology verification
Location/availability of FRM assessment	QA/maintenance	Guidance on transformation to satellite sensor	Ancillary data	Adequacy for class of instrument/measurand	Independent verification

**Table 12.** Grading criteria for the Maturity Matrix in Table 11.

Grade
Basic
Good
Excellent
Ideal

Concerning other criteria currently assessed as Good, more efforts will be needed to progressively meet higher class criteria and ultimately reach class A. To this aim, special attention will be brought to the following actions:

- Improve access to necessary ancillary data and complementary measurements. For MAX-DOAS measurements, the ideal configuration is to collocate instruments with sun photometers providing ancillary data on aerosol optical properties.
- Further develop the documentation on instruments, especially for non-commercial ones and make it available on the service website. Likewise, we will work on establishing systematic calibration and maintenance reports for all instruments.
- In the current state of the service, the set of instruments served by FRM4DOAS already covers a wide range of latitudes as well as different levels of pollution. When working



on the extension of the network, attention will be paid to prioritise measurement sites outside of Europe to progressively reach a better geographical coverage.

- The methodology to transform atmospheric composition FRM data into values comparable to satellite measurements has been documented in the peer-reviewed literature. We will make this information easily accessible through the service through dedicated training information.
- Along the same lines, we will also improve and better document the uncertainty estimates of the FRM data, make more explicit usage of the GUM approach and adopt the systematic usage of traceability chains.

In its current state of development, FRM4DOAS falls under class C according to the definition of the CEOS-FRM classification guidelines. As can be judged from Table 11, it already meets many of the key criteria. We are on the way to gradually reaching class B and, eventually, class A status over the next few years. This will be possible as part of the operationalisation and extension of the service planned between 2025 and 2028.

## 5. Conclusions and Outlook

Complementing other ground-based remote sensing atmospheric composition monitoring networks, such as AERONET [66] or PGN, the NDACC MAX-DOAS UV-Visible network focuses on measurements of trace gases in the troposphere. Although instruments and QA/QC procedures comply with quality standards imposed by the NDACC, e.g., through participation in regular intercalibration campaigns, efforts to harmonise retrieval methods and data production were limited, and for this reason, NDACC MAX-DOAS measurements did not strictly comply with the requirements formulated within QA4EO and imposed by the CEOS and space agencies to qualify as Fiducial Reference Measurements, i.e., reference measurements that meet the needs of the satellite community. For this reason, the NDACC UV-Vis working group, supported by ESA, initiated, in late 2016, the FRM4DOAS project. Based on a consortium of expert scientists having demonstrated knowledge in MAX-DOAS instrument calibration and operation, data retrieval methods and large-scale automated data processing, the first central data processing system for MAX-DOAS type instruments delivering quality-controlled trace gas and aerosol data products with a time latency of 1 day was developed. This system incorporates advanced retrieval algorithms for lower tropospheric and stratospheric NO<sub>2</sub> vertical profiles, formaldehyde vertical profiles and total ozone columns, selected by community consensus following a round-robin protocol. Its design is highly modular, which enables the seamless integration of new tools or algorithm updates as well as its upscaling to enable the progressive integration of a large number of stations (up to about 100 instruments).

During the first phase of the project, various activities took place including system design and implementation, performance assessment and various demonstration studies for satellite validation and model comparisons. A special emphasis was put on assessing the reliability of the generated data products through comparisons with results from alternative retrieval algorithms as well as independent measurements. Currently underway, the second R&D phase of the project focuses on improving existing algorithms and developing new ones, more specifically for cloud detection and classification, NO<sub>2</sub> measurements in urban areas and aerosol measurements. We also work on extending the system to generate a network-based stratospheric BrO data product, which would uniquely be available from FRM4DOAS.

In its current state, the FRM4DOAS service has been funded up to a demonstrational status, implying a limited capacity of processing and operation (restricted to the NRT data stream) but full functionality in terms of level-2 data delivery to the NDACC rapid delivery (RD) database and support to level-1 data providers. Currently, FRM4DOAS integrates 22 stations and delivers daily total ozone and tropospheric NO<sub>2</sub> profile datasets to the NDACC RD repository. As part of the service expansion planned from 2025 onwards, we intend to operationalise the retrieval of HCHO profiles and extend data processing at existing stations to provide historical datasets. At some sites, these data cover more than

20 years of observations. We also intend to progressively ingest data from a larger number of sites, thus improving the spatial coverage and representativeness of the network.

In the longer term, further extensions to the service may be envisaged. These include the retrieval of aerosol extinction, cloud information, stratospheric BrO profiles and NO<sub>2</sub> columns in urban environments. These products are currently being developed as part of the FRM4DOAS-2.0 R&D project. Further extensions could involve the retrieval of other gases of interest for satellite validation, such as glyoxal (CHOCHO), SO<sub>2</sub>, OClO or water vapour. In addition to satellite validation, the generation of such data products could serve many different applications, such as the assessment of three-dimensional chemical transport model outputs, analysis of variability and trends in composition, detection of pollution events and so on.

The FRM4DOAS service recently went through a CEOS-FRM self-assessment process aiming at assessing its compliance against a set of criteria addressing instrumentation, operations, data sampling, metrology and verification. The purpose was to evaluate where the current system is mature and where evolution and effort are still necessary. Based on this exercise, FRM4DOAS falls under class C according to the CEOS-FRM definition, which is a good score but also implies that improvements are needed to reach full compliance with FRM standards, i.e., class A. In the future, efforts will mainly concentrate on further operationalising the service and extending the number of stations and instruments being integrated into the processing system. The FRM4DOAS centralised data processing system will also constitute an essential element of the ACTRIS Centre for Reactive Trace Gases Remote Sensing (CREGARS, <https://www.actris.eu/index.php/topical-centre/cregars>, accessed on 27 November 2024), which includes a service to MAX-DOAS instruments operated at ACTRIS Reactive Trace Gases Remote Sensing National Facilities.

**Author Contributions:** Conceptualisation, M.V.R., F.H., M.M.F. and C.F.; methodology, F.H., M.M.F., C.F., M.V.R., U.F., A.R., T.W. and S.B.; software, M.M.F., C.F. and S.B.; validation, A.R., M.M.F., T.B., A.M. and G.P.; formal analysis, M.M.F., U.F., J.-L.T., T.B. and L.R.; investigation, M.M.F., U.F., J.-L.T., F.H., A.P., A.R., K.K. and T.W.; resources, S.B., U.F., M.N.C., O.P., M.Y., D.K., C.P.-R., S.Z., T.W., A.R., A.P. and A.M.; data curation, C.F., M.M.F. and F.H.; writing—original draft preparation, M.V.R., M.M.F., U.F., A.M., G.P., A.R., T.W., D.K., C.P.-R., O.P. and M.N.C.; writing—review and editing, M.V.R., A.B. and all; visualisation, M.M.F., M.V.R., D.K., U.F., G.P. and A.M.; supervision, F.H.; project administration, F.H., M.M.F. and M.V.R.; funding acquisition, M.V.R. All authors have read and agreed to the published version of the manuscript.

**Funding:** This research and APC were funded by the European Space Agency's FRM Programme under grant agreement no. 4000118181/16/I-EF (FRM4DOAS) and 4000135355/21/I-DT-Ir (FRM4DOAS 2.0). It was also supported by the ACTRIS European Research Infrastructure within its CREGARS Topical Centre as well as by the Belgian Federal Science Policy (Belspo) through the ACTRIS-BE project (contract no. FSIRI/00/AC1).

**Data Availability Statement:** The FRM4DOAS level-2 products of total ozone and NO<sub>2</sub> columns and profiles are available from the NDACC rapid delivery data repository at <https://www-air.larc.nasa.gov/missions/ndacc/data.html?RapidDelivery=rd-list>, accessed on 27 November 2024.

**Acknowledgments:** The authors wish to thank all the scientists and operators involved in the instrument development, operation and data analysis that made the FRM4DOAS project possible. INTA's team acknowledges the support of the Spanish Ministry of Science through the different research projects that have allowed long-term observations from Izaña. We also thank Angelika Dehn and Paolo Castracane from the European Space Agency for their continuous support of this project and their contributions to various meetings and discussions.

**Conflicts of Interest:** Author Karin Kreher was employed by the company BK Scientific. The remaining authors declare that the research was conducted in the absence of any commercial or financial relationships that could be construed as a potential conflict of interest.

## References

1. Burrows, J.P.; Weber, M.; Buchwitz, M.; Rozanov, V.; Ladstatter-Weissenmayer, A.; Richter, A.; de Beek, R.; Hoogen, R.; Bramstedt, K.; Eichmann, K.-U.; et al. The Global Ozone Monitoring Experiment (GOME): Mission Concept and First Scientific Results. *J. Atmos. Sci.* **1999**, *1*, 151–175. [CrossRef]
2. Bovensmann, H.; Burrows, J.P.; Buchwitz, M.; Frerick, J.; Noël, S.; Rozanov, V.V.; Chance, K.V.; Goede, A.P.H. SCIAMACHY: Mission Objectives and Measurement Modes. *J. Atmos. Sci.* **1999**, *56*, 127–150. [CrossRef]
3. Levelt, P.F.; Joiner, J.; Tamminen, J.; Veefkind, J.P.; Bhartia, P.K.; Stein Zweers, D.C.; Duncan, B.N.; Streets, D.G.; Eskes, H.; van der, A.R.; et al. The Ozone Monitoring Instrument: Overview of 14 years in space. *Atmos. Chem. Phys.* **2018**, *18*, 5699–5745. [CrossRef]
4. Munro, R.; Lang, R.; Klaes, D.; Poli, G.; Retscher, C.; Lindstrot, R.; Huckle, R.; Lacan, A.; Grzegorski, M.; Holdak, A.; et al. The GOME-2 instrument on the Metop series of satellites: Instrument design, calibration, and level 1 data processing—An overview. *Atmos. Meas. Tech.* **2016**, *9*, 1279–1301. [CrossRef]
5. Veefkind, J.P.; Aben, I.; McMullan, K.; Förster, H.; de Vries, J.; Otter, G.; Claas, J.; Eskes, H.J.; de Haan, J.F.; Kleipool, Q.; et al. TROPOMI on the ESA Sentinel-5 Precursor: A GMES mission for global observations of the atmospheric composition for climate, air quality and ozone layer applications. *Remote Sens. Environ.* **2012**, *120*, 70–83. [CrossRef]
6. Herman, J.R.; Cede, A.; Spinei, E.; Mount, G.; Tzortziou, M.; Abuhassan, N. NO<sub>2</sub> column amounts from ground-based Pandora and MFDOAS spectrometers using the direct-sun DOAS technique: Intercomparisons and application to OMI validation. *J. Geophys. Res.* **2009**, *114*, D13307. [CrossRef]
7. Hönninger, G.; Platt, U. Observations of BrO and its vertical distribution during surface ozone depletion at Alert. *Atmos. Environ.* **2002**, *36*, 2481–2489. [CrossRef]
8. Hönninger, G.; von Friedeburg, C.; Platt, U. Multi axis differential optical absorption spectroscopy (MAX-DOAS). *Atmos. Chem. Phys.* **2004**, *4*, 231–254. [CrossRef]
9. PETERS, A.J.M.; Boersma, K.F.; Kroon, M.; Hains, J.C.; Van Roozendaal, M.; Wittrock, F.; Abuhassan, N.; Adams, C.; Akrami, M.; Allaart, M.A.F.; et al. The Cabauw Intercomparison campaign for Nitrogen Dioxide measuring Instruments (CINDI): Design, execution, and early results. *Atmos. Meas. Tech.* **2012**, *5*, 457–485. [CrossRef]
10. Kreher, K.; Van Roozendaal, M.; Hendrick, F.; Apituley, A.; Dimitropoulou, E.; Frieß, U.; Richter, A.; Wagner, T.; Lampel, J.; Abuhassan, N.; et al. Intercomparison of NO<sub>2</sub>, O<sub>4</sub>, O<sub>3</sub> and HCHO slant column measurements by MAX-DOAS and zenith-sky UV-visible spectrometers during CINDI-2. *Atmos. Meas. Tech.* **2020**, *13*, 2169–2208. [CrossRef]
11. Pommereau, J.P.; Goutail, F. O<sub>3</sub> and NO<sub>2</sub> ground-based measurements by visible spectrometry during Arctic winter and spring 1988. *Geophys. Res. Lett.* **1988**, *15*, 891–894. [CrossRef]
12. Hendrick, F.; Barret, B.; Van Roozendaal, M.; Boesch, H.; Butz, A.; De Mazière, M.; Goutail, F.; Hermans, C.; Lambert, J.-C.; Pfeilsticker, K.; et al. Retrieval of nitrogen dioxide stratospheric profiles from ground-based zenith-sky UV-visible observations: Validation of the technique through correlative comparisons. *Atmos. Chem. Phys.* **2004**, *4*, 2091–2106. [CrossRef]
13. Hendrick, F.; Pommereau, J.-P.; Goutail, F.; Evans, R.D.; Ionov, D.; Pazmino, A.; Kyrö, E.; Held, G.; Eriksen, P.; Dorokhov, V.; et al. NDACC/SAOZ UV-visible total ozone measurements: Improved retrieval and comparison with correlative ground-based and satellite observations. *Atmos. Chem. Phys.* **2011**, *11*, 5975–5995. [CrossRef]
14. Donner, S.; Kuhn, J.; Van Roozendaal, M.; Bais, A.; Beirle, S.; Bösch, T.; Bogner, K.; Bruchkouski, I.; Chan, K.L.; Dörner, S.; et al. Evaluating different methods for elevation calibration of MAX-DOAS (Multi AXis Differential Optical Absorption Spectroscopy) instruments during the CINDI-2 campaign. *Atmos. Meas. Tech.* **2020**, *13*, 685–712. [CrossRef]
15. Schreier, S.F.; Richter, A.; Peters, E.; Ostendorf, M.; Schmalwieser, A.W.; Weihs, P.; Burrows, J.P. Dual ground-based MAX-DOAS observations in Vienna, Austria: Evaluation of horizontal and temporal NO<sub>2</sub>, HCHO, and CHOCHO distributions and comparison with independent data sets. *Atmos. Environ.* **2020**, *5*, 100059. [CrossRef]
16. Dimitropoulou, E.; Hendrick, F.; Pinardi, G.; Friedrich, M.M.; Merlaud, A.; Tack, F.; De Longueville, H.; Fayt, C.; Hermans, C.; Laffineur, Q.; et al. Validation of TROPOMI tropospheric NO<sub>2</sub> columns using dual-scan multi-axis differential optical absorption spectroscopy (MAX-DOAS) measurements in Uccle, Brussels. *Atmos. Meas. Tech.* **2020**, *13*, 5165–5191. [CrossRef]
17. Rodgers, C.D. *Inverse Methods for Atmospheric Sounding, Theory and Practice*; World Scientific Publishing: Singapore; Hackensack, NJ, USA; London, UK; Hong Kong, China, 2000; Available online: [https://www.worldscientific.com/worldscibooks/10.1142/3171?srsltid=AfmBOorfOa6\\_jROgPxPqWXMgSNYk-Q4F9cw7t9H7YSoqJrZv3eLZJpVh#t=aboutBook](https://www.worldscientific.com/worldscibooks/10.1142/3171?srsltid=AfmBOorfOa6_jROgPxPqWXMgSNYk-Q4F9cw7t9H7YSoqJrZv3eLZJpVh#t=aboutBook) (accessed on 27 November 2024).
18. Clémer, K.; Van Roozendaal, M.; Fayt, C.; Hendrick, F.; Hermans, C.; Pinardi, G.; Spurr, R.; Wang, P.; De Mazière, M. Multiple wavelength retrieval of tropospheric aerosol optical properties from MAX-DOAS measurements in Beijing. *Atmos. Meas. Tech.* **2010**, *3*, 863–878. [CrossRef]
19. Bösch, T.; Rozanov, V.; Richter, A.; Peters, E.; Rozanov, A.; Wittrock, F.; Merlaud, A.; Lampel, J.; Schmitt, S.; de Haij, M.; et al. BOREAS—A new MAX-DOAS profile retrieval algorithm for aerosols and trace gases. *Atmos. Meas. Tech.* **2018**, *11*, 6833–6859. [CrossRef]
20. Frieß, U.; Monks, P.; Remedios, J.; Rozanov, A.; Sinreich, R.; Wagner, T.; Platt, U. MAX-DOAS O<sub>4</sub> measurements: A new technique to derive information on atmospheric aerosols: 2. Modeling studies. *J. Geophys. Res.* **2006**, *111*, D14203. [CrossRef]
21. Friedrich, M.M.; Rivera, C.; Stremme, W.; Ojeda, Z.; Arellano, J.; Bezanilla, A.; García-Reynoso, J.A.; Grutter, M. NO<sub>2</sub> vertical profiles and column densities from MAX-DOAS measurements in Mexico City. *Atmos. Meas. Tech.* **2019**, *12*, 2545–2565. [CrossRef]

22. Wang, Y.; Li, A.; Xi, P.-H.; Chen, H.; Xu, J.; Wu, F.-C.; Liu, J.-G.; Liu, W.-Q. Retrieving vertical profile of aerosol extinction by multi-axis differential optical absorption spectroscopy. *Acta Phys. Sin.* **2013**, *62*, 180705. [CrossRef]
23. Beirle, S.; Dörner, S.; Donner, S.; Remmers, J.; Wang, Y.; Wagner, T. The Mainz profile algorithm (MAPA). *Atmos. Meas. Tech.* **2019**, *12*, 1785–1806. [CrossRef]
24. Vlemmix, T.; Piters, A.J.M.; Berkhout, A.J.C.; Gast, L.F.L.; Wang, P.; Levelt, P.F. Ability of the MAX-DOAS method to derive profile information for NO<sub>2</sub>: Can the boundary layer and free troposphere be separated? *Atmos. Meas. Tech.* **2011**, *4*, 2659–2684. [CrossRef]
25. Frieß, U.; Beirle, S.; Alvarado Bonilla, L.; Bösch, T.; Friedrich, M.M.; Hendrick, F.; Piters, A.; Richter, A.; van Roozendaal, M.; Rozanov, V.V.; et al. Intercomparison of MAX-DOAS vertical profile retrieval algorithms: Studies using synthetic data. *Atmos. Meas. Tech.* **2019**, *12*, 2155–2181. [CrossRef]
26. Danckaert, T.; Fayt, C.; Van Roozendaal, M.; De Smedt, I.; Letocard, V.; Merlaud, A.; Pinaridi, G. QDOAS Software User Manual, Version 3.2. 2017. Available online: [http://uv-vis.aeronomie.be/software/QDOAS/QDOAS\\_manual.pdf](http://uv-vis.aeronomie.be/software/QDOAS/QDOAS_manual.pdf) (accessed on 24 March 2024).
27. Chance, K.; Kurucz, R.L. An improved high-resolution solar reference spectrum for earth's atmosphere measurements in the ultraviolet, visible, and near infrared. *J. Quant. Spectrosc. Radiat. Transf.* **2010**, *111*, 1289–1295. [CrossRef]
28. Serdyuchenko, A.; Gorshelev, V.; Weber, M.; Chehade, W.; Burrows, J.P. High spectral resolution ozone absorption cross-sections—Part 2: Temperature dependence. *Atmos. Meas. Tech.* **2014**, *7*, 625–636. [CrossRef]
29. Vandaele, A.C.; Hermans, C.; Simon, P.C.; Carleer, M.; Colin, R.; Fally, S.; Mérianne, M.-F.; Jenouvrier, A.; Coquart, B. Measurements of the NO<sub>2</sub> absorption cross section from 42000 cm<sup>-1</sup> to 10000 cm<sup>-1</sup> (238–1000 nm) at 220 K and 294 K. *J. Quant. Spectrosc. Radiat. Transf.* **1998**, *59*, 171–184. [CrossRef]
30. Thalman, R.; Volkamer, R. Temperature dependent absorption cross-sections of O<sub>2</sub>-O<sub>2</sub> collision pairs between 340 and 630 nm and at atmospherically relevant pressure. *Phys. Chem. Phys.* **2013**, *15*, 15371–15381. [CrossRef]
31. Rothman, L.S.; Gordon, I.E.; Babikov, Y.; Barbe, A.; Chris Benner, D.; Bernath, P.F.; Birk, M.; Bizzocchi, L.; Boudon, V.; Brown, L.R.; et al. The HITRAN2012 molecular spectroscopic database. *J. Quant. Spectrosc. Radiat. Transf.* **2013**, *130*, 4–50. [CrossRef]
32. Chance, K.V.; Spurr, R.J.D. Ring effect studies: Rayleigh scattering, including molecular parameters for rotational Raman scattering, and the Fraunhofer spectrum. *Appl. Opt.* **1997**, *36*, 5224. [CrossRef]
33. Wagner, T.; Beirle, S.; Deutschmann, T. Three-dimensional simulation of the Ring effect in observations of scattered sun light using Monte Carlo radiative transfer models. *Atmos. Meas. Tech.* **2009**, *2*, 113–124. [CrossRef]
34. Preston, K.E.; Jones, R.L.; Roscoe, H.K. Retrieval of NO<sub>2</sub> vertical profiles from ground-based UV-visible measurements: Method and validation. *J. Geophys. Res.* **1997**, *102*, 19089–19097. [CrossRef]
35. Errera, Q.; Fonteyn, D. Four-dimensional variational chemical assimilation of CRISTA stratospheric measurements. *J. Geophys. Res.* **2001**, *106*, 12253–12265. [CrossRef]
36. Chipperfield, M.P. New version of the TOMCAT/SLIMCAT off-line chemical transport model: Intercomparison of stratospheric tracer experiments. *Q. J. R. Meteorol. Soc.* **2006**, *132*, 1179–1203. [CrossRef]
37. Kylling, A.; Mayer, B. LibRadTran: A Package for UV and Visible Radiative Transfer Calculations in the Earth's Atmosphere. 2003. Available online: <https://www.libradtran.org> (accessed on 27 November 2024).
38. Hendrick, F.; Van Roozendaal, M.; Kylling, A.; Petritoli, A.; Rozanov, A.; Sanghavi, S.; Schofield, R.; von Friedeburg, C.; Wagner, T.; Wittrock, F.; et al. Intercomparison exercise between different radiative transfer models used for the interpretation of ground-based zenith-sky and multi-axis DOAS observations. *Atmos. Chem. Phys.* **2006**, *6*, 93–108. [CrossRef]
39. Wagner, T.; Burrows, J.P.; Deutschmann, T.; Dix, B.; Von Friedeburg, C.; Frieß, U.; Hendrick, F.; Heue, K.P.; Irie, H.; Iwabuchi, H.; et al. Comparison of box-air-mass-factors and radiances for multiple-axis differential optical absorption spectroscopy (MAX-DOAS) geometries calculated from different UV/visible radiative transfer models. *Atmos. Chem. Phys.* **2007**, *7*, 1809–1833. [CrossRef]
40. Wang, Y.; Lampel, J.; Xie, P.; Beirle, S.; Li, A.; Wu, D.; Wagner, T. Ground-based MAX-DOAS observations of tropospheric aerosols, NO<sub>2</sub>, SO<sub>2</sub> and HCHO in Wuxi, China, from 2011 to 2014. *Atmos. Chem. Phys.* **2017**, *17*, 2189–2215. [CrossRef]
41. Takashima, H.; Irie, H.; Kanaya, Y.; Shimizu, A.; Aoki, K.; Akimoto, H. Atmospheric aerosol variations at Okinawa Island in Japan observed by MAX-DOAS using a new cloud-screening method. *J. Geophys. Res. Atmos.* **2009**, *114*, D18213. [CrossRef]
42. Gielen, C.; Van Roozendaal, M.; Hendrick, F.; Pinaridi, G.; Vlemmix, T.; De Bock, V.; De Backer, H.; Fayt, C.; Hermans, C.; Gillotay, D.; et al. A simple and versatile cloud-screening method for MAX-DOAS retrievals. *Atmos. Meas. Tech.* **2014**, *7*, 3509–3527. [CrossRef]
43. Wagner, T.; Apituley, A.; Beirle, S.; Dörner, S.; Friess, U.; Remmers, J.; Shaiganfar, R. Cloud detection and classification based on MAX-DOAS observations. *Atmos. Meas. Tech.* **2014**, *7*, 1289–1320. [CrossRef]
44. Wang, Y.; Penning de Vries, M.; Xie, P.H.; Beirle, S.; Dörner, S.; Remmers, J.; Li, A.; Wagner, T. Cloud and aerosol classification for 2.5 years of MAX-DOAS observations in Wuxi (China) and comparison to independent data sets. *Atmos. Meas. Tech.* **2015**, *8*, 5133–5156. [CrossRef]
45. Wagner, T.; Beirle, S.; Remmers, J.; Shaiganfar, R.; Wang, Y. Absolute calibration of the colour index and O<sub>4</sub> absorption derived from Multi AXis (MAX-)DOAS measurements and their application to a standardised cloud classification algorithm. *Atmos. Meas. Tech.* **2016**, *9*, 4803–4823. [CrossRef]

46. Koelemeijer, R.B.A.; de Haan, J.F.; Stammes, P. A database of spectral surface reflectivity in the range 335–772 nm derived from 5.5 years of GOME observations. *J. Geophys. Res.* **2003**, *108*, 4070. [CrossRef]
47. Barthia, P.K.; Wellemeyer, C.G.; Taylor, S.L.; Nath, N.; Gopalan, A. Solar Backscatter (SBUV) Version 8 profile algorithm. In Proceedings of the Quadrennial Ozone Symposium 2004, Athens, Greece, 1–8 June 2004; Zerefos, C., Ed.; pp. 295–296, ISBN 960-630-103-6.
48. Anderson, G.P.; Clough, S.A.; Kneizys, F.X.; Chetwynd, J.H.; Shettle, E.P. *AFGL (Air Force Geophysical Laboratory) Atmospheric Constituent Profiles (0. 120km), Environmental Research Papers*; Air Force Geophysics Laboratory, Hanscom AFB: Lincoln, MA, USA, 1986.
49. Hendrick, F.; Fayt, C.; Friedrich, M.M.; Frieß, U.; Richter, A.; Beirle, S.; Wagner, T.; Wang, Y. MAXDOAS Algorithm Theoretical Baseline Document, FRM4DOAS Deliverable D6. Available online: [https://frm4doas.aeronomie.be/ProjectDir/Deliverables/FRM4DOAS\\_D6\\_MAXDOAS\\_Algorithm\\_ATBD\\_v02\\_20180130.pdf](https://frm4doas.aeronomie.be/ProjectDir/Deliverables/FRM4DOAS_D6_MAXDOAS_Algorithm_ATBD_v02_20180130.pdf) (accessed on 27 November 2024).
50. Tirpitz, J.-L.; Frieß, U.; Hendrick, F.; Alberti, C.; Allaart, M.; Apituley, A.; Bais, A.; Beirle, S.; Berkhout, S.; Bognar, K.; et al. Intercomparison of MAX-DOAS vertical profile retrieval algorithms: Studies on field data from the CINDI-2 campaign. *Atmos. Meas. Tech.* **2021**, *14*, 1–35. [CrossRef]
51. Wagner, T.; Beirle, S.; Benavent, N.; Bösch, T.; Chan, K.L.; Donner, S.; Dörner, S.; Fayt, C.; Frieß, U.; García-Nieto, D.; et al. Is a scaling factor required to obtain closure between measured and modelled atmospheric O<sub>4</sub> absorptions? An assessment of uncertainties of measurements and radiative transfer simulations for 2 selected days during the MADCAT campaign. *Atmos. Meas. Tech.* **2019**, *12*, 2745–2817. [CrossRef]
52. Apituley, A.; Kreher, K.; Van Roozendaal, M.; Sullivan, J.; McGee, T.J.; Allaart, M.; PETERS, A.; Stein, D.C.; Eskes, H.; Henzing, J.S.; et al. Overview of activities during the 2019 TROPOMI validation experiment (TROLIX'19). In Proceedings of the AGU Fall Meeting 2019, San Francisco, CA, USA, 9–13 December 2019; Available online: <https://agu.confex.com/agu/fm19/meetingapp.cgi/Paper/521767> (accessed on 27 November 2024).
53. Lange, K.; Richter, A.; Schönhardt, A.; Meier, A.C.; Bösch, T.; Seyler, A.; Krause, K.; Behrens, L.K.; Wittrock, F.; Merlaud, A.; et al. Validation of Sentinel-5P TROPOMI tropospheric NO<sub>2</sub> products by comparison with NO<sub>2</sub> measurements from airborne imaging DOAS, ground-based stationary DOAS, and mobile car DOAS measurements during the S5P-VAL-DE-Ruhr campaign. *Atmos. Meas. Tech.* **2023**, *16*, 1357–1389. [CrossRef]
54. Bae, K.; Song, C.-K.; Van Roozendaal, M.; Richter, A.; Wagner, T.; Merlaud, A.; Pinardi, G.; Friedrich, M.M.; Fayt, C.; Dimitropoulou, E.; et al. Validation of GEMS operational v2.0 Total Column NO<sub>2</sub> and HCHO during the GMAP/SIJAQ campaign. *Science of the Total Environment*, manuscript number: STOTEN-D-24-42580 (under review).
55. Lange, K.; Richter, A.; Bösch, T.; Zilker, B.; Latsch, M.; Behrens, L.K.; Okafor, C.M.; Bösch, H.; Burrows, J.P.; Merlaud, A.; et al. Validation of GEMS tropospheric NO<sub>2</sub> columns and their diurnal variation with ground-based DOAS measurements. *Atmos. Meas. Tech.* **2024**, *17*, 6315–6344. [CrossRef]
56. Pinardi, G.; Van Roozendaal, M.; Hendrick, F.; Theys, N.; Abuhassan, N.; Bais, A.; Boersma, F.; Cede, A.; Chong, J.; Donner, S.; et al. Validation of tropospheric NO<sub>2</sub> column measurements of GOME-2A and OMI using MAX-DOAS and direct sun network observations. *Atmos. Meas. Tech.* **2020**, *13*, 6141–6174. [CrossRef]
57. Verhoelst, T.; Compernelle, S.; Pinardi, G.; Lambert, J.-C.; Eskes, H.J.; Eichmann, K.-U.; Fjæraa, A.M.; Granville, J.; Niemeijer, S.; Cede, A.; et al. Ground-based validation of the Copernicus Sentinel-5P TROPOMI NO<sub>2</sub> measurements with the NDACC ZSL-DOAS, MAX-DOAS and Pandora global networks. *Atmos. Meas. Tech.* **2021**, *14*, 481–510. [CrossRef]
58. Oomen, G.-M.; Müller, J.-F.; Stavrou, T.; De Smedt, I.; Blumenstock, T.; Kivi, R.; Makarova, M.; Palm, M.; Röhling, A.; Té, Y.; et al. Weekly derived top-down volatile-organic-compound fluxes over Europe from TROPOMI HCHO data from 2018 to 2021. *Atmos. Chem. Phys.* **2024**, *24*, 449–474. [CrossRef]
59. Yombo Phaka, R.; Merlaud, A.; Pinardi, G.; Friedrich, M.M.; Van Roozendaal, M.; Müller, J.-F.; Stavrou, T.; De Smedt, I.; Hendrick, F.; Dimitropoulou, E.; et al. Ground-based Multi-AXIS Differential Optical Absorption Spectroscopy (MAX-DOAS) observations of NO<sub>2</sub> and H<sub>2</sub>CO at Kinshasa and comparisons with TROPOMI observations. *Atmos. Meas. Tech.* **2023**, *16*, 5029–5050. [CrossRef]
60. Van Geffen, J.; Eskes, H.; Compernelle, S.; Pinardi, G.; Verhoelst, T.; Lambert, J.-C.; Snee, M.; ter Linden, M.; Ludewig, A.; Boersma, K.F.; et al. Sentinel-5P TROPOMI NO<sub>2</sub> retrieval: Impact of version v2.2 improvements and comparisons with OMI and ground-based data. *Atmos. Meas. Tech.* **2022**, *15*, 2037–2060. [CrossRef]
61. Irie, H.; Takashima, H.; Kanaya, Y.; Boersma, K.F.; Gast, L.; Wittrock, F.; Brunner, D.; Zhou, Y.; Van Roozendaal, M. Eight-component retrievals from ground-based MAX-DOAS observations. *Atmos. Meas. Tech.* **2011**, *4*, 1027–1044. [CrossRef]
62. Kanaya, Y.; Irie, H.; Takashima, H.; Iwabuchi, H.; Akimoto, H.; Sudo, K.; Gu, M.; Chong, J.; Kim, Y.J.; Lee, H.; et al. Long-term MAX-DOAS network observations of NO<sub>2</sub> in Russia and Asia (MADRAS) during the period 2007–2012: Instrumentation, elucidation of climatology, and comparisons with OMI satellite observations and global model simulations. *Atmos. Chem. Phys.* **2014**, *14*, 7909–7927. [CrossRef]
63. Kumar, V.; Beirle, S.; Dörner, S.; Mishra, A.K.; Donner, S.; Wang, Y.; Sinha, V.; Wagner, T. Long-term MAX-DOAS measurements of NO<sub>2</sub>, HCHO, and aerosols and evaluation of corresponding satellite data products over Mohali in the Indo-Gangetic Plain. *Atmos. Chem. Phys.* **2020**, *20*, 14183–14235. [CrossRef]

64. Lee, G.T.; Park, R.J.; Kwon, H.-A.; Ha, E.S.; Lee, S.D.; Shin, S.; Ahn, M.-H.; Kang, M.; Choi, Y.-S.; Kim, G.; et al. First evaluation of the GEMS formaldehyde retrieval algorithm against TROPOMI and ground-based column measurements during the in-orbit test period. *EGUsphere* **2023**. preprint. [[CrossRef](#)]
65. Goryl, P.; Fox, N.; Donlon, C.; Castracane, P. Fiducial reference measurements (FRMs): What are they? *Remote Sens.* **2023**, *15*, 5017, ISSN 2072-4292. [[CrossRef](#)]
66. Giles, D.M.; Sinyuk, A.; Sorokin, M.G.; Schafer, J.S.; Smirnov, A.; Slutsker, I.; Eck, T.F.; Holben, B.N.; Lewis, J.R.; Campbell, J.R.; et al. Advancements in the Aerosol Robotic Network (AERONET) Version 3 database—Automated near-real-time quality control algorithm with improved cloud screening for Sun photometer aerosol optical depth (AOD) measurements. *Atmos. Meas. Tech.* **2019**, *12*, 169–209. [[CrossRef](#)]

**Disclaimer/Publisher’s Note:** The statements, opinions and data contained in all publications are solely those of the individual author(s) and contributor(s) and not of MDPI and/or the editor(s). MDPI and/or the editor(s) disclaim responsibility for any injury to people or property resulting from any ideas, methods, instructions or products referred to in the content.